frontiers in Materials

REVIEW
published: 28 June 2021
doi: 10.3389/fmats.2021.692309

Mesoporous Silica Based Nanostructures for Bone Tissue Regeneration

Sougata Ghosh[1†]* *and Thomas J. Webster*[2†]

[1]*Department of Microbiology, School of Science, RK University, Rajkot, India,* [2]*Department of Chemical Engineering, Northeastern University, Boston, MA, United States*

Porous nano-scaffolds provide for better opportunities to restore, maintain, and improve functions of damaged tissues and organs by facilitating tissue regeneration. Various nanohybrids composed of mesoporous silica nanoparticles (MSNs) are being widely explored for tissue engineering. Since biological activity is enhanced by several orders of magnitude in multicomponent scaffolds, remarkable progress has been observed in this field, which has aimed to develop the controlled synthesis of multifunctional MSNs with tuneable pore size, efficient delivering capacity of bioactive factors, as well as enhanced biocompatibility and biodegradability. In this review, we aim to provide a broad survey of the synthesis of multifunctional MSN based nanostructures with exotic shapes and sizes. Further, their promise as a novel nanomedicine is also elaborated with respect to their role in bone tissue engineering. Also, recent progress in surface modification and functionalization with various polymers like poly (L-lactic acid)/poly (ε-caprolactone), polylysine-modified polyethylenimine, poly (lactic-co-glycolic acid), and poly (citrate-siloxane) and biological polymers like alginate, chitosan, and gelatine are also covered. Several attempts for conjugating drugs like dexamethasone and β–estradiol, antibiotics like vancomycin and levofloxaci, and imaging agents like fluorescein isothiocyanate and gadolinium, on the surface modified MSNs are also covered. Finally, the scope of developing orthopaedic implants and potential trends in 3D bioprinting applications of MSNs are also discussed. Hence, MSNs based nanomaterials may serve as improved candidate biotemplates or scaffolds for numerous bone tissue engineering, drug delivery and imaging applications deserving our full attention now.

Keywords: porous nanostructures, nanohybrids, polymers, multifunctional scaffolds, drug delivery, bioimaging, 3D bioprinting

OPEN ACCESS

Edited by:
Juan Valerio Cauich-Rodriguez, Centro de Investigación Científica de Yucatán, A.C. (CICY), Mexico

Reviewed by:
Jennifer Patterson, Instituto IMDEA Materiales, Spain
Rajendra Kumar Singh, Institute of Tissue Regeneration Engineering (ITREN), South Korea

***Correspondence:**
Sougata Ghosh
ghoshsibb@gmail.com

†ORCID:
Sougata Ghosh
orcid.org/0000-0003-0077-1318
Thomas J. Webster
orcid.org/0000-0002-2028-5969

Specialty section:
This article was submitted to Biomaterials, a section of the journal Frontiers in Materials

Received: *08 April 2021*
Accepted: *28 May 2021*
Published: *28 June 2021*

Citation:
Ghosh S and Webster TJ (2021) Mesoporous Silica Based Nanostructures for Bone Tissue Regeneration. Front. Mater. 8:692309. doi: 10.3389/fmats.2021.692309

INTRODUCTION

The recent past has witnessed a tremendous advancement in the area of orthopaedic surgery and development of bone implants considering the growing number of cases of traumatic injury, tumors, deformity, degeneration and an age related ailments. The limitations of the traditional synthetic porous scaffolds which are often made out of metals, polymers, ceramics or even composite biomaterials, include incompatibility with native tissue structure and properties of bone tissues. This leads to poor integration of the synthetic scaffolds with cells and surrounding host tissue, thereby resulting in unsatisfactory surgical outcomes due to poor corrosion and wear, mechanical mismatch, unamiable surface environments, and other unfavorable properties (Wu et al., 2014).

Among various tissues, bone is the most notable due to its role in the support of other tissues, locomotion, hematopoiesis, protection, calcium and phosphate balance and also structural integrity (Florencio-Silva et al., 2015). It is estimated that the cumulative annual cost for the treatment of almost 15 million patients in the United States with bone disorders, 1.6 million traumatic fractures, and 2 million osteoporosis associated bone defects is about $45 billion (O'Keefe and Mao, 2011). Depending upon the severity of the damage and absence of a full proof healing strategy, bone grafting has increased tremendously as an alternative therapeutic strategy chosen by approximately 1.6 million patients in the United States alone annually incurring costs of around $2.5 billion (Amini et al., 2012; Bao et al., 2013).

Conventional therapy for fixing bone defects has various limitations, such as a shortage of grafts and donors; surgical procedure associated bleeding, pain, morbidity, and post surgical infections; and a failure in osseointegration and graft rejection have been emphasized as the immediate need to develop complementary and alternative therapies for bone injuries (Yaszemski et al., 1996; Finkemeier, 2002; Dimitriou et al., 2011; Mishra et al., 2016).

In view of this background, nanotechnology driven bone tissue engineering approaches have gained global attention over the past decade for developing cost effective, durable, and biocompatible implants or scaffolds (Hickey et al., 2015). The main objectives of orthopaedic surgery include the reconstruction of musculoskeletal tissue that can be achieved by i) prosthetic or fixation device and ii) tissue engineered bone scaffolds. Hence, choosing the ideal biomaterial with enhanced porosity, better tensile strength and longer shelf life has attracted wide attention in nanotechnological research. Materials such as bioactive glasses, carbon nanostructures, and hydroxyapatite nanoparticles are widely-proposed hard materials for the repair and regeneration of bone related wounds and "delicate" structures in the body. These materials are advantageous as they can improve cell proliferation and differentiation, enhance angiogenesis, and can possess antibacterial/anti- inflammatory activities (Kargozar et al., 2020).

Mesoporous silica nanoparticles (MSNs) with high porosity provide an ambient microenvironment for cell adherence, proliferation and differentiation (Perez et al., 2017). Similarly, associating MSNs with metallic materials, e.g., 316L stainless steel, titanium alloys and cobalt chromium alloys, can enhance the load-bearing capacity of prostheses. Functionalization of scaffolds with ligands like bone morphogenetic proteins (BMPs) and drugs like dexamethasone (DEX) help in osteoinduction and differentiation of osteoprogenitor cells, particularly mesenchymal stem cells (MSCs) (Dragonas et al., 2019).

In this review, advances in the fabrication of novel mesoporous silica based nanomaterials for bone repair is discussed in detail. Furthermore, the role and mechanism of biomaterials in ensuring rapid healing, efficient vascularization, proper osseointegration and blood supply are also elaborated. These biomaterial based implants with longer shelf lives and reasonable costs may help to ensure a tissue regenerative microenvironment resembling the natural extracellular matrix (ECM) of bone itself.

OSTEOGENESIS

Bone tissue is derived from MSCs which exhibit promising abilities like self repair, regrowth and remodelling. For the most part, MSCs with intrinsic self-renewal properties remain in an "undifferentiated" state unless stimulated. Although MSCs are mostly isolated from bone marrow, alternate sources can be peripheral blood, gingiva tissue, adipose tissue, skeletal muscle, tendons, neonatal umbilical cord blood and specific parts of the placenta. MSCs positively express CD105 (SH3), CD90, and CD73 (SH2) while negatively express CD34, CD45, CD14 or CD11b, CD79α, or CD19 and HLA-DR. Multipotent MSCs can further differentiate into osteoblasts, chondrocytes, and adipocytes upon the right stimulation (Dominici et al., 2006).

Various induction factors are required to promote the differentiation of MSCs into osteocytes. Certain supplements, when added to the basal medium, can induce osteogenesis. Similarly, hydrostatic pressure, mechanical stress and a pulsed electromagnetic field (PEMF) can also facilitate osteogenic differentiation (Hess et al., 2010; Jansen et al., 2010; Yourek et al., 2010). It is interesting to note that the supplementation of dexamethasone in the basal medium can remarkably stimulate *in vitro* osteogenesis which is attributed to the up-regulated expression of the runt-related transcription factor 2 (Runx2), Osterix (Osx), and bone morphogenetic proteins (BMPs) (Igarashi et al., 2004). Similarly, ascorbic acid and β-glycerophosphate enhance the secretion of type I collagen which is a hallmark of osteogenesis (Gupta et al., 2007).

Various factors mediate the osteogenic pathway at different steps as seen in **Figure 1**. The most notable marker, Runx2, controls the initial steps where osteogenic differentiation of MSCs is activated either by transforming growth factor-beta 1 (TGF β1) or bone morphogenetic protein 2 (BMP2) pathways (Lee et al., 2000; Lee et al., 2003). Runx2 also plays a vital role in inhibiting MSCs to differentiate into an adipogenic lineage thus promoting the commitment of MSCs specifically to the osteogenic lineage along with both BMP2 and distal-less homeobox 5 (Dlx5) (Enomoto et al., 2004; Gaur et al., 2005). Runx2 independent Osx expression is mediated by BMP2 and preosteoblasts are formed that can further express Runx2, D1x5, msh homeobox homologue 2 (Msx2), P2Y4 and P2Y14 (Harada and Rodan, 2003). A low expression of osteoblast specific markers like alkaline phosphatase (ALP), type I collagen (collagen I), and osteopontin (OPN) may be observed at this stage. The formation of immature osteoblasts from preosteoblasts is facilitated by β-catenin, Runx2, and Osx (Komori, 2006). Spindle shaped immature osteoblasts express bone matrix proteins such as bone sialoprotein and OPN (Komori, 2006). Osx mediates the terminal maturation of osteoblasts with the induction of osteocalcin (OC) expression while the maturation of osteoblasts is inhibited by Runx2 (Liu et al., 2001; Nakashima et al., 2002). Upon complete differentiation into osteoblasts, mature cells exhibit a mineralized matrix, cuboidal shape, well

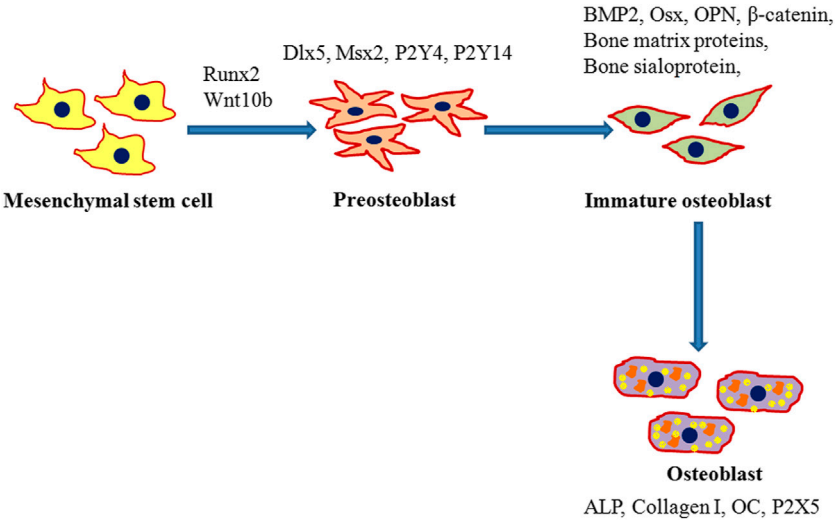

FIGURE 1 | Schematic representation for the differentiation of mesenchymal stem cells (MSCs) into osteoblasts. Runx2 mediated commitment of MSCs to an osteogenic lineage followed by the initial formation of preosteoblasts that express runt-related transcription factor 2 (Runx2), distal-less homeobox 5 (Dlx5), and msh homeobox homologue 2 (Msx2). Preosteoblasts further differentiate into immature osteoblasts which in turn enhance expression of bone morphogenetic protein 2 (BMP2), Osterix (Osx), β-catenin, bone matrix proteins, bone sialoprotein, and osteopontin (OPN) and develop into mature osteoblasts. Mature osteoblasts with a mineralized cellular matrix express osteocalcin (OC), alkaline phosphatase (ALP), and type I collagen (collagen I).

developed Golgi bodies and rough endoplasmic reticulum. The enhanced expression of P2X5, ALP, collagen I and OC is observed in mature osteoblasts (Pavlin et al., 2000; Pavlin et al., 2001).

Numerous porous biomaterials are constantly being fabricated and functionalized with bioactive ligands in order to promote the osteogenic differentiation of MSCs as listed in **Table 1**. Thus, porous nanomaterials can be an attractive alternative to existing solid metallic implants which can not only mimic the tissue micro environment but also would provide suitable mechanical strength and durability. Based on their chemistry, size, and geometry, mesoporous silica based nanoparticles are the most preferred nanostructures that can be used for enhancing bone repair and regeneration.

MESOPOROUS SILICA NANOPARTICLES

Although nanotechnology has made tremendous progress in the domain of healthcare over the past decades, there is a continual need to combine novel nanostructures with scaffolds that can mimic the tissue micro-environment and natural extracellular matrix. Such an approach is a prerequisite to develop nanomaterial based tissue engineering strategies and stem cell therapies for tissue regeneration (Padmanabhan and Kyriakides, 2015). The unique properties of mesoporous silica nanoparticles (MSNs), like high specific surface area, tunable morphology and pore size, multi-functionalizability, and enhanced biocompatibility have made them ideal nanomaterials for bone tissue engineering (Croissant et al., 2018). Functionalized MSNs can respond effectively to a plethora of stimuli like temperature, pH, light, redox potential and enzymes that make them the most suitable nanocarriers for targeted drug delivery and triggered release (Rahikkala et al., 2018). Several contrast agents can be conjugated on/in the MSNs for effective bioimaging that help in monitoring their biodistribution, accumulation and organ specific targeting (Henstock et al., 2015; Chen et al., 2019).

Zhou et al. (2015) reported the fabrication of fluorescein isothiocyanate (FITC)-labeled MSNs after surface modification and expression of amine groups by a treatment with 3-aminopropyltriethoxysilane (APTES) as shown in **Figure 2**. Further, the BMP-2 peptides (79.8%) were functionalized by a covalent interaction between –COOH and $-NH_2$ groups resulting in cross-linking. Although the hydrodynamic diameter of the bare MSNs was 265 nm with a polydispersity index (PDI) of 0.196, after peptide functionalization, the MSN-pep exhibited a smaller hydrodynamic diameter of 255 nm and a narrower PDI of 0.172. This indicated a better dispersion and stability of MSN-pep that might have been attributed to the peptide grafting. Enhanced cellular uptake of MSN-pep in a time dependent manner was evident in bone mesenchymal stem cells (BMSCs) when treated from 24 to 48 h. ALP activity of the cells treated with DEX conjugated BMP-2 peptide functionalized MSNs (DEX@MSNs-pep) was maximal on the 14th day. Similarly, high calcium deposition in the cells was confirmed upon treatment with DEX@MSNs-pep. Also, expression of RUNX2 and OCN was enhanced due to treatment with the multifunctionalized nanocomposite. **Figure 2E** depicts ectopic bone formation after 3 weeks indicating the osteogenic capacity of MSNs-pep and DEX@MSNs-pep. Upon implantation of the nanocomposites, the post-operation CT images confirmed the calcified deposits in the MSNs-pep and DEX@MSNs-pep treatment groups. Bone mineralization was also facilitated by the DEX@MSNs-pep compared to the MSNs-pep only.

TABLE 1 | The application of MSNs as scaffolds for bone tissue engineering.

Nanomaterial	Functionalized ligands/drugs	Size (nm)	Examined cell line	Advantages	Disadvantages	Refs
Mesoporous silica nanoparticles (MSNs)	Fluorescein isothiocyanate (FITC), bone morphogenetic protein-2 (BMP-2), dexamethasone (DEX)	255	Bone mesenchymal stem cells	Better dispersion, high osteoinductive effect	Unknown biodistribution and excretion profile	Zhou et al. (2015)
Collagen (col) with bioactive glass nanocarriers (BGn)	FGF18	—	Rat bone mesenchymal stem cells	Sustained release of functionalized biomolecule	Targeting and resistance to biofouling is absent	Mahapatra et al. (2016)
Polycaprolactone shelled with mesoporous silica (PCL@MS)	Cytochrome *c*, doxorubicin, gentamycin sulphate, and fluorescein isothiocyanate	422 ± 97	Rat bone marrow mesenchymal stem cells	Superior nanomechanical surface property and sustained release	Shelf life and stability is unknown	Singh et al. (2015)
Poly (L-lactic acid)/poly (ε-caprolactone) (PLLA/PCL) nanofibrous MSNs scaffold	Dexamethasone	318.8	Rat bone marrow mesenchymal stem cells	*In-vivo* bone healing and high collagen formation	Toxicity and biomagnification of MSN in the tissue is unclear	Qiu et al. (2016)
Titanium (Ti) substrate supported MSNs with multilayered hybrid chitosan/gelatin (CHI/Gel) pair	β–estradiol	180 ± 22	Osteoblasts isolated from neonatal rat calvaria	enhanced osteoblast proliferation and tissue regeneration	Resistance to microbial infections is unclear	Hu et al. (2010)
Chitosan-functionalized MSNs	Bone morphogenetic protein-2, dexamethasone	130	Rat bone marrow mesenchymal stem cells	Dual delivery of drug and BMP-2	Optimization and release study should be performed	Gan et al. (2015)
Polylysine-modified polyethylenimine (PEI-PLL) and arginine-glycine-aspartate (RGD) functionalized MSNs	Dexamethasone, bone morphogenetic protein-2 pDNA	<200	Bone mesenchymal stem cells	Dual drug and DNA delivery	Functionalized DNA might not be stable for longer duration	Zhou et al. (2019)
True bone ceramics (TBC) combined with hollow MSNs (TBC/HMSN/P28)	Chitosan	—	MC3T3-E1 cells	Sustained release property, excellent biocompatibility, and strong bone conduction and regeneration ability.	Healing time may take long due to absence of functionalized precursors or osteoinductive drugs	Cui et al. (2018)
Alginate/chitosan (ALG/CHI), poly-L-lactide (PLLA), poly (lactic-co-glycolic acid) (PLGA)-conjugated MSNs	Sphingosine-1-phosphate, BMP-2	119.82 ± 8.80	Rat bone marrow mesenchymal stem cells	Simultaneous osteogenic and angiogenic activities	Long term side effects and biocompatibility is unknown	Zhang et al. (2018)
Poly (L-lactide) (PLLA) oligomer based novel biodegradable polyester modified MSNs	—	200–350	MC3T3-E1 cells	Promotion of cell viability, proliferation and tissue repair	Unknown pharmacokinetics and pharmaco-dynamics	Wang et al. (2019)
Gadolinium (Gd) labelled defect-related luminescent MSN	Dexamethasone	100	Bone mesenchymal stem cells	Simultaneous bioimaging and drug delivery	Unknown adverse reactions	Ren et al. (2017)
Silica nanoparticles (SNs) reinforced with poly (citrate-siloxane) hybrid elastomers (PCS-SN)	—	500	MC3T3-E1	Simultaneous bioimaging and bone tissue regeneration	Shelf life and biodistribution pattern is not known	Li et al. (2018)
MSNs in gelatin matrix	Vancomycin	209.8	Rat bone marrow mesenchymal stem cells	Dual antimicrobial and osteogenic activities	Functionalization of single antibiotic might not be able to inhibit multidrug resistant pathogens	Zhou et al. (2018)
Mesoporous silica microspheres/nanohydroxyapatite/polyurethane composite scaffold	Levofloxacin	—	Chronic osteomyelitis animal model using New Zealand White rabbits	Dual treatment for pathogenic infection and osteomyelitis	Durability and biocompatibility should be investigated	Wang et al. (2017)
Calcium phosphate cement (CPC)-based mesoporous silica scaffolds	Recombinant human bone morphogenic protein-2 (rhBMP-2)	—	Human bone marrow stromal cells	Simultaneous promotion of both promote both vascularization and osteogenesis	The 3D bioprinting technique can be expensive and time consuming	Li et al. (2017)

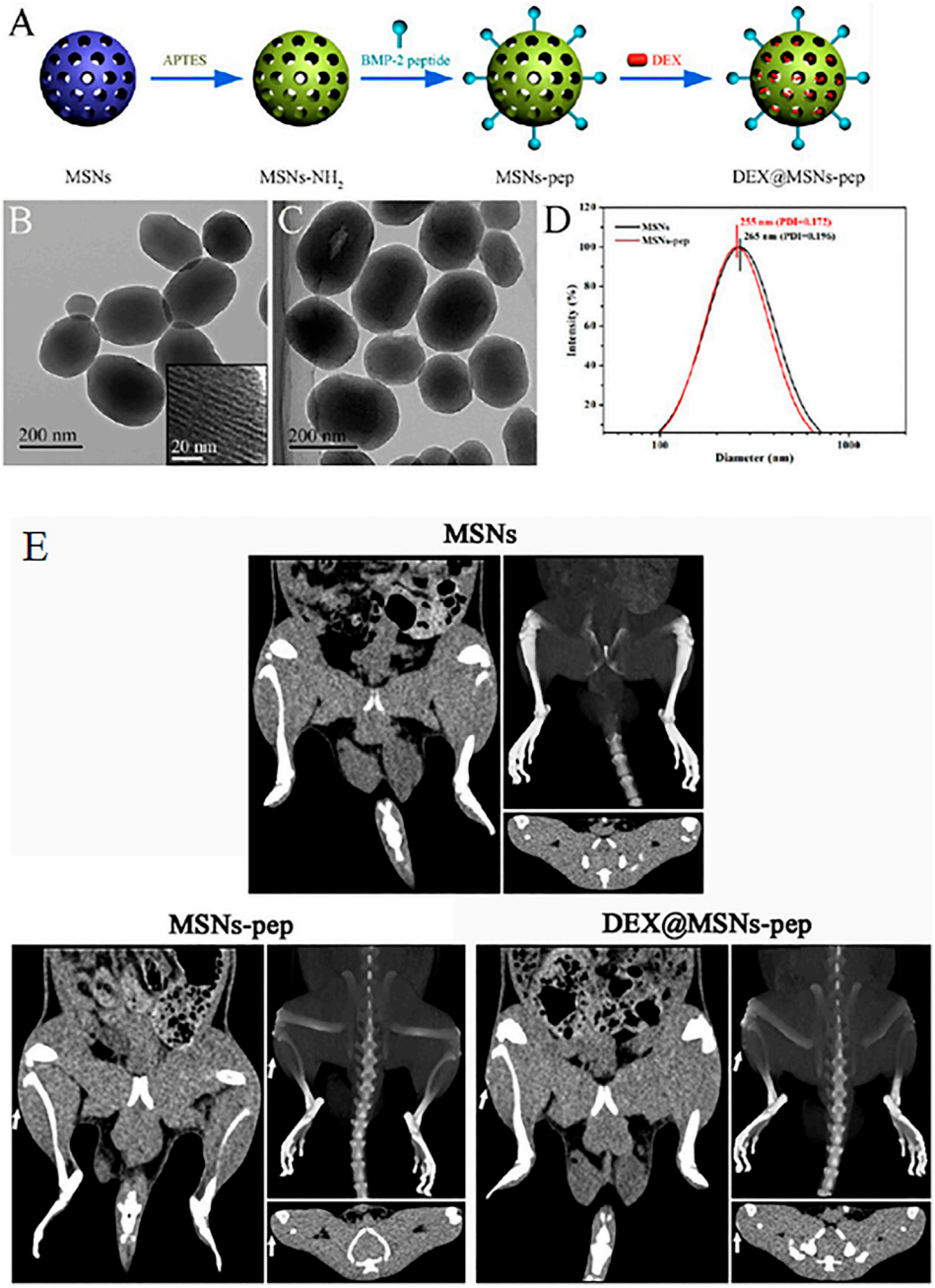

FIGURE 2 | (A) Schematic illustration for the preparation of DEX@MSNs-pep; TEM images of **(B)** MSNs (inset is the enlarged image) and **(C)** MSNs-pep; and **(D)** size distribution of MSNs and MSNs-pep. **(E)** CT images of rats implanted with different implants for 3 weeks. Images of (left) plain CT scanning, (upper right) three-dimensional CT reconstruction, and (bottom right) transverse section for each MSNs, MSNs-pep, and DEX@MSNs-pep. Reprinted with permission from Zhou et al. (2015). Copyright © 2015 American Chemical Society.

A critical factor controlling the biological response to MSNs is their morphology, particularly, the shape and size that also determines the extent of cellular uptake. MSNs of smaller dimensions (50 nm) were reported to show better uptake when fluorescence-labeled MSNs of a controlled size in the range of 30–280 nm were incubated with HeLa cells (Lu et al., 2009). However, Vallhov et al. (2007) reported that larger MSNs showed selectively more uptake by the phagocytic cells compared to smaller ones. In view of this background, the appropriate tuneable size of MSNs seems to be a prerequisite for the better performance of MSNs in immune escape and cellular uptake.

Likewise, the shape of MSNs also plays a critical role in cell adhesion, cell uptake, biodistribution and clearance (Huang et al.,

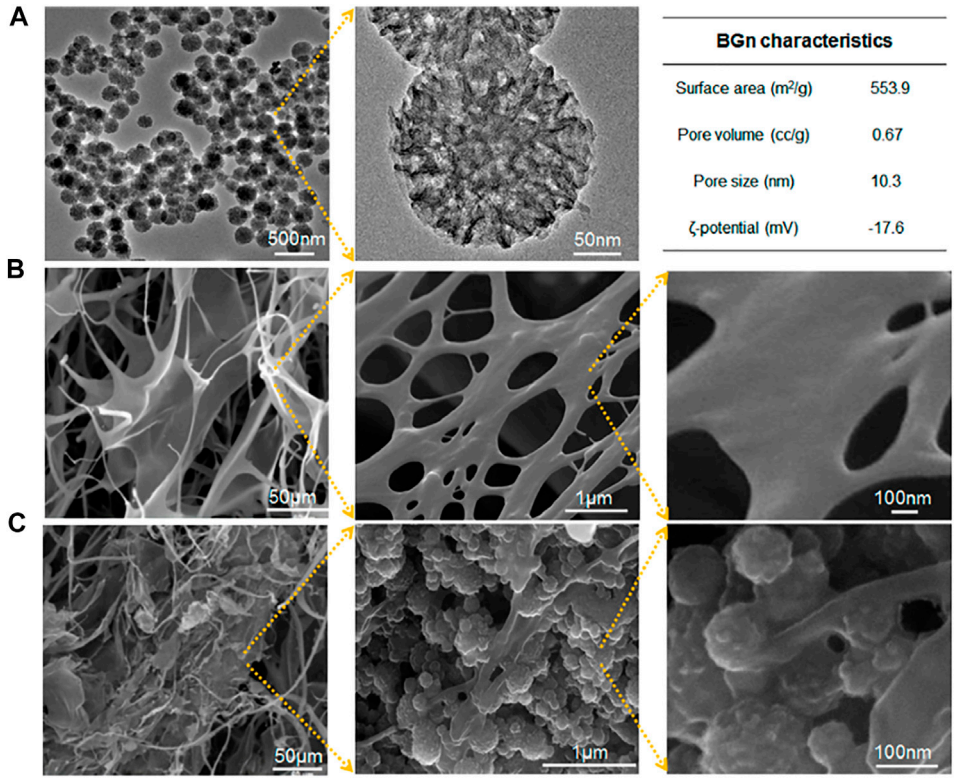

FIGURE 3 | Characteristics of BGn and BGn/Col gel. **(A)** TEM images of BGn at different magnifications with characteristics summarized. **(B,C)** SEM images of freeze-dried gels at different magnifications: **(B)** Col and **(C)** BGn/Col. Reprinted with permission from Mahapatra et al. (2016). Copyright © 2016, American Chemical Society.

2010; Huang et al., 2011). Larger MSNs (with aspect ratios AR = 4) were internalized in A375 human melanoma cells. Interestingly, short-rod MSNs were more rapidly cleared than long-rod MSNs. Therefore, the above findings indicated that optimizing the size and shape of MSNs is of great importance before incorporating them into scaffolds for bone tissue regeneration.

POLYMER FUNCTIONALIZED MESOPOROUS SILICA NANOCOMPOSITES

Numerous polymers have been functionalized on the surface of MSNs to provide biomatrices for the efficient anchorage of stem cells, promotion of cellular growth, migration, and lineage differentiation. Hydrogels made out of biopolymers like gelatine, collagen, chitosan, etc., can encapsulate cells and provide a 3D environment that largely mimics the native tissue extracellular matrix (ECM). MSNs can be incorporated into such polymers to fabricate novel osteogenic scaffolds that can be directly delivered to the damaged tissue space with minimal invasiveness.

Mahapatra et al. (2016) designed a stem cell delivering gel matrix made of collagen (Col) with bioactive glass nanocarriers (BGn) that was co-functionalized with an osteogenic signaling molecule, fibroblast growth factor 18 (FGF18), within the mesopore structure. The Col/BGn hydrogel exhibited remarkable enhanced osteogenic differentiation of mesenchymal stem cells (MSCs) that was attributed to the release of ions. **Figure 3** illustrates the mesopores within the BGn that is advantageous for effective loading of FGF18 at large quantities. Similarly, the nanoarchitecture also helped in the sustained release of FGF18 from the BGn-Col gel matrix with almost a zero-order kinetics, over 4 weeks. The release of FGF18 enhanced MSC alkaline phosphatase activity and upregulated bone related gene expression along with bone matrix formation (osteopontin, bone sialoprotein, and osteocalcin production). Hence, this FGF18-BGn/Col gel can be a promising osteo-promoting scaffold for bone tissue engineering.

Similarly, in another study, Singh et al. (2015) fabricated a novel nanofibrous hybrid scaffold of polycaprolactone shelled with mesoporous silica (PCL@MS) as shown in **Figure 4**. This nanocomposite possessed dual advantages where the silica shell served as an active biointerface and the 3D nanoscale fibrous structure acted as a cell-stimulating matrix. Together they enhanced bone regeneration. Upon coating the electrospun PCL nanofibers with MS, surface wettability and ionic reactions improved significantly resulting in the substantial

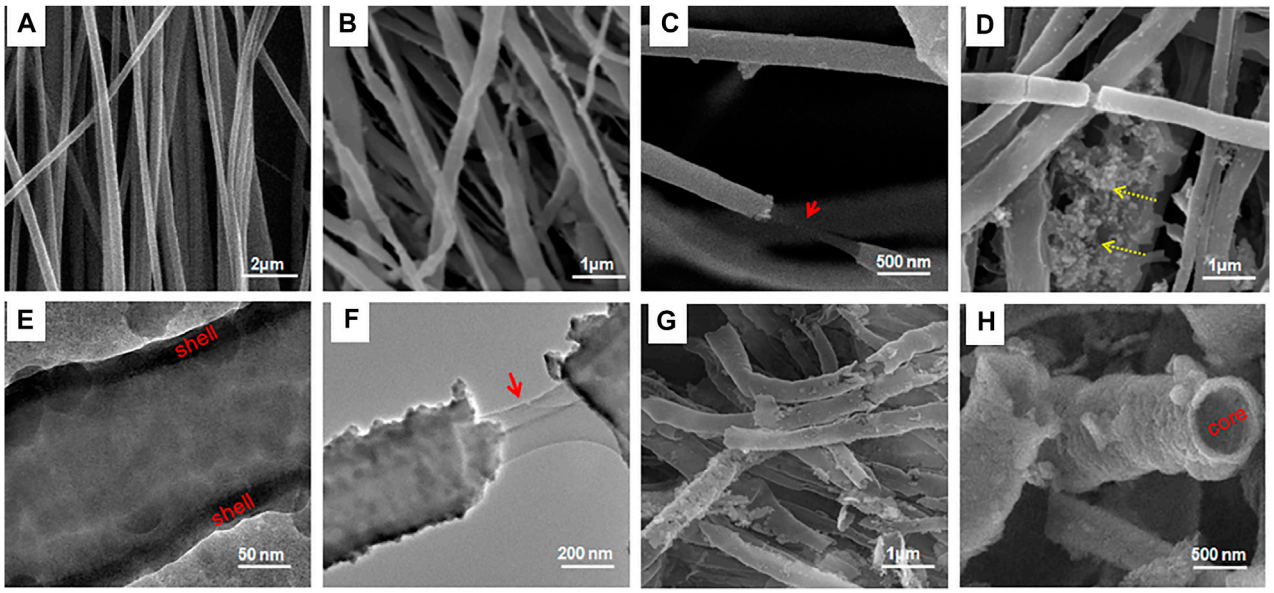

FIGURE 4 | Morphology and other characteristics of PCL@MS hybrid nanofibers: **(A–D,G,H)** SEM and **(E,F)** TEM images of the samples. **(A)** PCL used as a template (422 ± 97 nm in size); **(B)** after one coating cycle, PCL@MS induced a homogeneous coverage of the silica layer on the surface; **(C)** morphology stretching showing the inner PCL (arrow) and outer silica layer; **(D)** when the coating cycle was exceeded (twice), some precipitates of the silica nanoparticles appeared (dotted arrows); **(E)** TEM image clearly showing the silica layer forming uniformly on the surface (indicated as "shell"); **(F)** nanofiber stretching revealing the inner PCL (arrow) and the outer silica layer; **(G,H)** SEM image of the thermally treated PCL@MS, with complete removal of the inner PCL core (indicated as "core"), revealing a hollow MS structure. Reprinted with permission from Singh et al. (2015). Copyright © 2015 American Chemical Society.

formation of bone-like mineral apatite in body-simulated medium. The hybrid nanofibers exhibited superior mechanical properties, such as tensile strength and elastic modulus. The excellent nanomechanical surface properties of the nanomaterial favored hard tissue repair where rat MSCs had better attachment, growth, and proliferation. Interestingly, the nanohybrid stimulated the *ALP* and *Col I* genes to their highest level at the 14th day, while the expression of *OPN* and *OCN* genes were the highest on day 21, indicating time-dependent gene expression. Further, the high loading capacity of cytochrome c (cyt C), doxorubicin (DOX), gentamycin sulphate (GS), and fluorescein isothiocyanate (FITC) on the surface of PCL@MS nanofibers showed their promising role as theranostic agents. A sustained release was observed for all four biomolecules from the nanocomposite surface supporting its prolonged activity.

Qiu et al. (2016) reported aminated mesoporous silica nanoparticles (MSNs-NH_2) as efficient microcarriers for dexamethasone (DEX). Initially, a thermally induced phase separation (TIPS) technique was employed for the synthesis of poly (L-lactic acid)/poly (ε-caprolactone) (PLLA/PCL) nanofibrous scaffold onto which the DEX-loaded MSNs-NH_2 nanoparticles (DEX@MSNs-NH_2) were deposited by electrophoretic deposition (EPD) as illustrated in **Figure 5A**. About 8.09% DEX was loaded onto the DEX@MSNs-NH_2. The shape of the MSNs-NH_2 was mostly elliptical and uniform with a size of 318.8 nm while the pore diameter of the scaffold was approximately 15.66 μm. The DEX@MSNs-NH_2 particles were localized on the surface and within the pores of the scaffolds after deposition. Although a rapid DEX release from the scaffolds was evident in the beginning, it gradually slowed, and a sustained release was achieved with time. The DEX@MSNs-NH_2/PLLA/PCL facilitated an increase in cell numbers of primary rat bone marrow mesenchymal stem cells (BMSCs) from 3 to 14 days indicating their role in maintaining cell viability and promoting cell division. Interestingly, BMSCs not only grew and differentiated efficiently, but also collagen production, matrix mineralization and osteocalcin expression was enhanced when grown on the DEX@ MSNs-NH_2/PLLA/PCL scaffolds.

Further, the DEX@MSNs-NH2/PLLA/PCL scaffolds facilitated calvarial defect healing in Sprague–Dawley (SD) rats as represented in **Figure 5B**. Substantial bone healing was evident at 24 h as confirmed in 3D micro-CT imaging which might be attributed to the DEX release. In view of this background, MSNs based multifunctionalized nanoscaffolds can be considered as ideal candidates for the delivery of osteogenic agents to induce BMSCs differentiation and commitment to an osteogenic lineage.

Hu et al. (2010) reported that titanium (Ti) substrates supported MSN embedded in multilayered hybrid chitosan/gelatin (Chi/Gel) pairs. This composite served as a nanoreservoir-type drug delivery system that could regulate the growth of both osteoblasts and osteoclasts which is crucial for the maintenance of bone homeostasis. A layer-by-layer (LbL) assembly technique was employed to facilitate the electrostatic interactions of polyanions and polycations for fabricating the nanocomposite. Further, β –estradiol (E2) was used as a standard drug for loading since it is well known for its therapeutic applications for the amelioration of osteoporosis. Initially, the MSNs were used as nanoreservoirs for the loading of β–estradiol

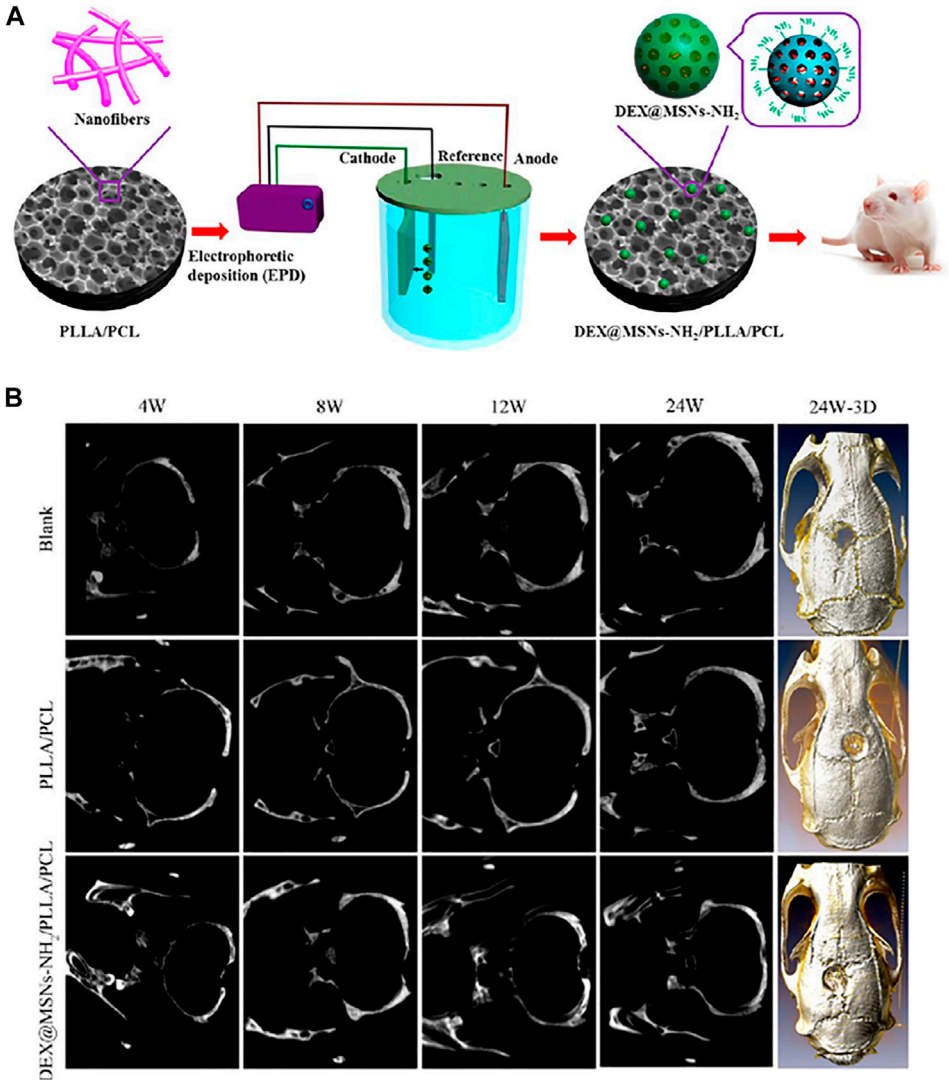

FIGURE 5 | (A) Schematic illustration for the fabrication of DEX@MSNs-NH2/PLLA/PCL composite scaffolds; **(B)** Micro-CT evaluation of SD rat calvarial bone defects. Images of plain micro-CT scanning at 4, 8, 12, and 24 W (left) and 3D micro-CT reconstruction after 24 W (right) of implantation of the blank and the PLLA/PCL and DEX@MSNs-NH_2/PLLA/PCL scaffolds. Reprinted with permission from Qiu et al. (2016). Copyright © 2016 American Chemical Society.

which were further coated with polyelectrolyte multilayers (PEM) of gelatin/chitosan (E2-MSN@PEM). Additionally, the E2-MSN@PEM nanoparticles were also embedded in between the Gel/Chi pair layers. The MSNs were spherical with an average diameter of 133 ± 16 nm. In the drug loaded composites, 7% of β –estradiol was loaded onto the MSNs. After coating with layers of $(Chi/Gel)_2/Chi$, the particle size of the E2-MSN@PEM nanoparticles increased to 180 ± 22 nm. Each layer was 4.7 nm thick. The effect of the nanocomposites was checked on osteoblasts isolated from neonatal rat calvaria employing a sequential collagenase digestion method. Superior cytocompatibility of the nanocomposite with an induction of strong mineralization after 16 days in osteoblasts confirmed their potential as promising agents in bone tissue engineering and bone regeneration with simultaneous drug delivery.

In another study, polymeric chitosan was used to develop MSN based nanocomposites with an enhanced osteoinductive effect. Dexamethasone (DEX) at a suitable dosage can enhance bone morphogenetic protein-2 (BMP-2) mediated osteoblast differentiation and accelerate bone regeneration. To strengthen this synergistic osteoinductive effect, a pH-responsive chitosan-functionalized mesoporous silica nanoparticle (chi-MSN) ensemble was fabricated for the dual-delivery of BMP-2 and DEX. Initially, a CTAB-templated sol-gel method was employed to synthesize MSNs 130 nm in diameter that were further reacted with glycidoxypropyltrimethoxysilane (GPTMS) for cross-linking chitosan. DEX was functionalized by encapsulation in the mesopores while the larger BMP-2 was localized within the chitosan coating. Rapidly released BMP-2 (over 80%) from the chi-MSNs was efficiently endocytosed while the lower pH values

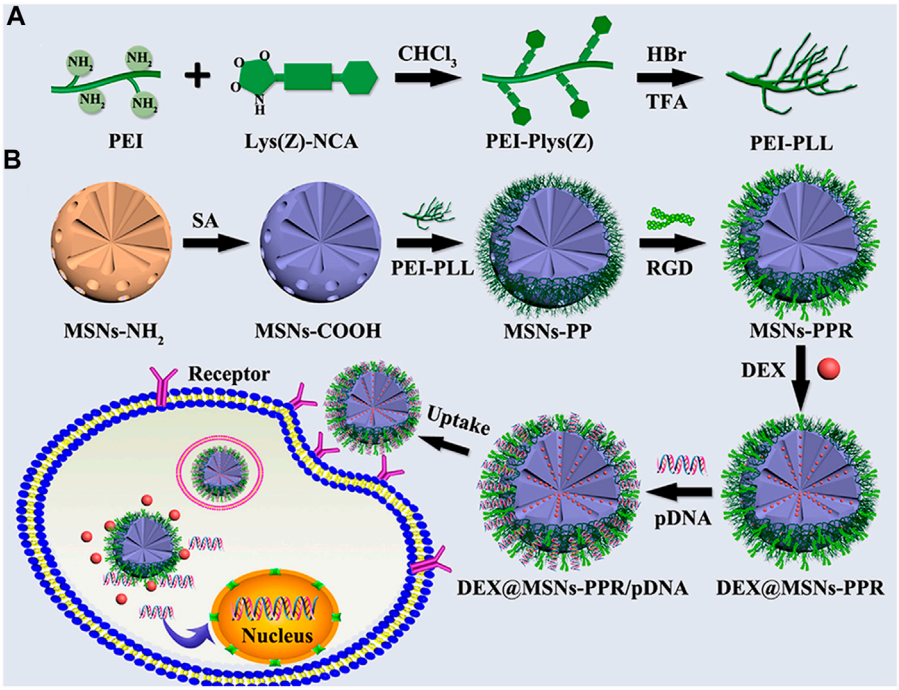

FIGURE 6 | (A) Reaction scheme for the synthesis of PEI-PLL copolymers. **(B)** Schematic illustration for the preparation of PEI-PLL and RGD-conjugated MSNs-based nanocarrier and codelivery of pDNA and drug into cells. Reprinted with permission from Zhou et al. (2019). Copyright © 2019 American Chemical Society.

within the cell, facilitated the controlled release of DEX. Superior osteoblast differentiation and bone regeneration upon treatment with this dual hybrid nanocomposite was attributed to the synergistic action of BMP-2 and DEX outside and inside the cell (Gan et al., 2015).

Zhou et al. (2019) reported the synthesis of polymer functionalized MSNs for the dual delivery of genes and drugs. Initially, polylysine-modified polyethylenimine (PEI-PLL) copolymers were synthesized with PEI of varying molecular weights. The PEI-PLL-25k (a copolymer synthesized using 25 kDa PEI) exhibited superior *in vitro* transfection efficiency and low cytotoxicity. Further, MSNs were surface functionalized with a PEI-PLL-25k copolymer and arginine-glycine-aspartate (RGD) peptide to facilitate the surface adsorption of plasmid DNA and loading of an osteogenic drug dexamethasone (DEX) in the mesopores as illustrated in **Figure 6.** The MSNs-NH_2 were mostly spherical with highly ordered mesoporous structures. RGD functionalization on the surface of the MSNs helped enhance cytocompatibility. The co-polymer based dual delivery system exhibited rapid release of plasmid DNA (pDNA). However, a sustained release of DEX was also observed. Bone mesenchymal stem cells (BMSCs) transfected with a vector bearing bone morphogenetic protein-2 (BMP-2) pDNA significantly increased expression of the BMP-2 protein. The novel dual-factor delivery system with DEX and the BMP-2 gene enhanced the osteogenic differentiation of BMSCs which was attributed to the upregulation of alkaline phosphatase (ALP) activity, expression of osteo-related genes, and calcium deposition as shown in **Figure 7**.

In another study, a nanocomposite was fabricated by Cui et al. (2018) in order to ensure the controlled release of a novel BMP-2-related peptide (designated P28) from chitosan (CHI) functionalized true bone ceramics (TBC) which was combined with an enlarged pore hollow mesoporous silica nanoparticle (HMSNs) composite scaffold (TBC/HMSN/P28). **Figure 8** schematically illustrates the synthesis strategy for the TBC/HMSN/P28 scaffold where initially TBC was reacted with 700 μL of a HMSN/P28 solution followed by vacuum drying for 30 min twice and then was kept at 4°C for 24 h before freeze-drying. A slow and sustained release of P28 from the nanocomposite scaffold was confirmed which helped in the superior proliferation and osteogenic differentiation of MC3T3-E1 cells. After four kinds of scaffolds were implanted into a rabbit radius critical bone defect for 6 and 12 weeks, the radiographic and histological examination indicated that this osteogenic delivery system, TBC/HMSN/P28 scaffolds, effectively induced bone regeneration *in vivo*. Therefore, the TBC/HMSN/P28 scaffold can promote the proliferation and osteogenic differentiation of MC3T3-E1 cells *in vitro* and new bone tissue generation *in vivo*. This study provides a promising scaffold for bone tissue engineering and regenerative medicine which should be further studied.

Improper vascularization may lead to non-unions in bones. Hence, it is crucial to develop biomaterials that can facilitate coordination between angiogenesis and osteogenesis. Zhang et al. (2018) fabricated a novel angiogenic carrier by loading sphingosine-1-phosphate (S1P) into mesoporous silica nanoparticles (MSNs). The microcarriers were then integrated

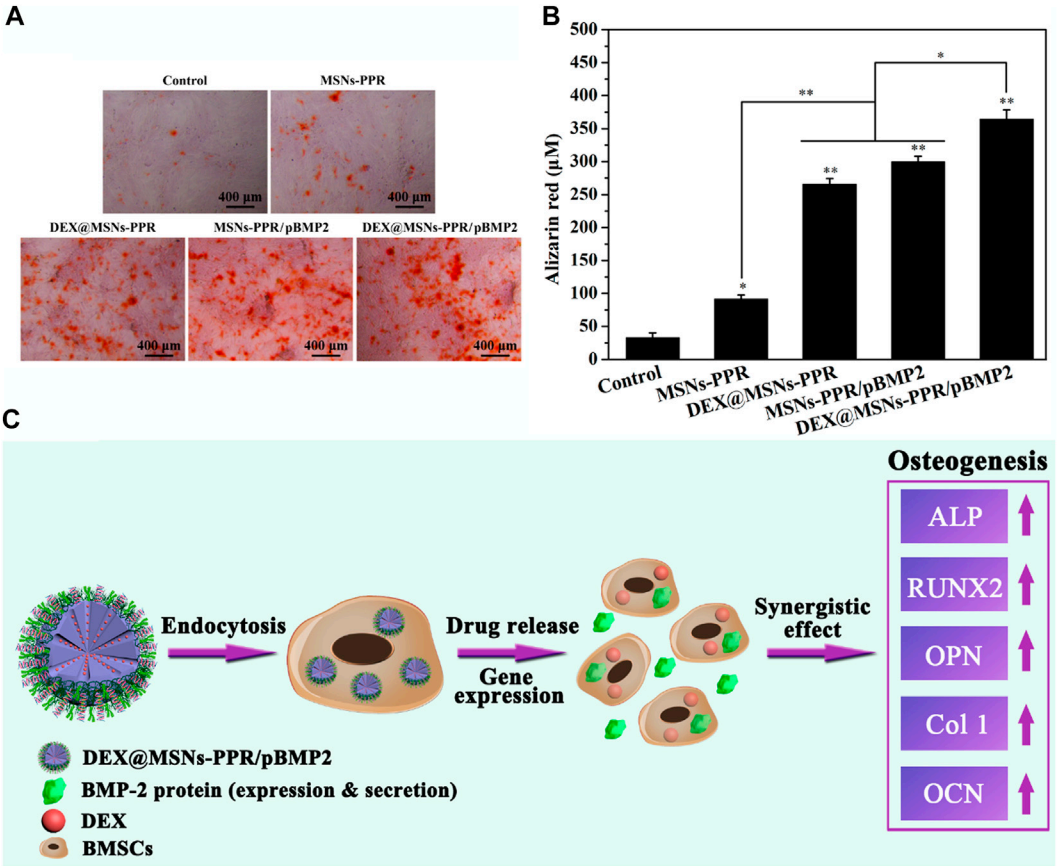

FIGURE 7 | Evaluation of the mineralization in BMSCs after incubation with different samples for 21 days **(A)** Digital photos of alizarin red S staining. **(B)** Quantitative analysis of mineralized matrix. **(C)** Schematic illustration of the osteogenic differentiation of BMSCs induced by the MSNs-based BMP-2 gene and DEX codelivery system. *$p < 0.05$ and **$p < 0.01$ against the control group. Reprinted with permission from Zhou et al. (2019). Copyright © 2019 American Chemical Society.

into porous nanofibrous poly-L-lactide (PLLA) scaffolds as shown in **Figure 9**. Further, poly (lactic-co-glycolic acid) (PLGA) microspheres were used for encapsulating the BMP-2 to develop osteogenic microcarriers, that were subsequently embedded into the MSNs/PLLA scaffolds.

Morphologically, the MSNs were spherical with a diameter of 108.05 ± 11.58 nm while functionalization with alginate/chitosan (ALG/CHI) increased the diameter to 119.82 ± 8.80 nm as seen in **Figure 10**. The PLGA microspheres synthesized by a double emulsion technique shown in **Figure 9B** were also spherical with an average diameter of 2.84 ± 0.99 mm. Further, the acMSNs/PLLA scaffold was fabricated using a sugar-leaching technique as demonstrated in **Figure 9C**. Rational variation in the size of the sugar sphere was used to control the pore diameter of the acMSNs/PLLA scaffold. The superior porosity of the material was attributed to the interconnected macropores and regular pore channels. Interestingly, a nanofibrous structure was seen inside the pore walls. PLGA microspheres were uniformly integrated with the acMSNs/PLLA scaffold.

Osteogenic activity was enhanced in BMSCs when grown on dual-bioactive factor containing scaffolds, namely BMP-2@PLGA/acMSNs/PLLA (G2) and BMP-2@PLGA/S1P@acMSNs/PLLA scaffolds (G3) for up to 7 days. The biocompatible scaffolds with BMP-2 facilitated the proliferation, spreading of the BMSCs and osteoinduction which was also associated with the significant enhancement of ALP activity and calcium nodule formation. Additionally, the dual-factor (BMP-2 and S1P) loaded scaffold (G3) induced remarkably high ectopic bone formation than the BMP-2 loaded scaffold (G2) within 8 weeks. A notable amount of mineralization with a bone shell formation surrounding the bone marrow cavity was observed upon treatment with (G3) confirming the superior osteogenic potential of the dual bioactive factor loaded porous nanofibrous scaffolds.

Wang et al. (2019) reported the synthesis of poly (L-lactide) (PLLA) oligomer based novel biodegradable polyester modified MSNs for bone tissue repair. Initially, a PLLA-TMC-GA terpolymer (PLTG) was synthesized by ring-opening polymerization at 130°C for 72 h using L-lactide (LLA)/trimethylene carbonate (TMC)/glycolide (GA) at a ratio of 90:5:5 in the presence of Sn $(Oct)_2$ as a catalyst. Modified mesoporous silica (MCM41) was synthesized which was further used for the fabrication of the PLTG/PLLA-MCM41 composite films employing solution casting. The resulting MCM41 particles were mostly spherical with sizes ranging from 200 to 350 nm. The PLLA

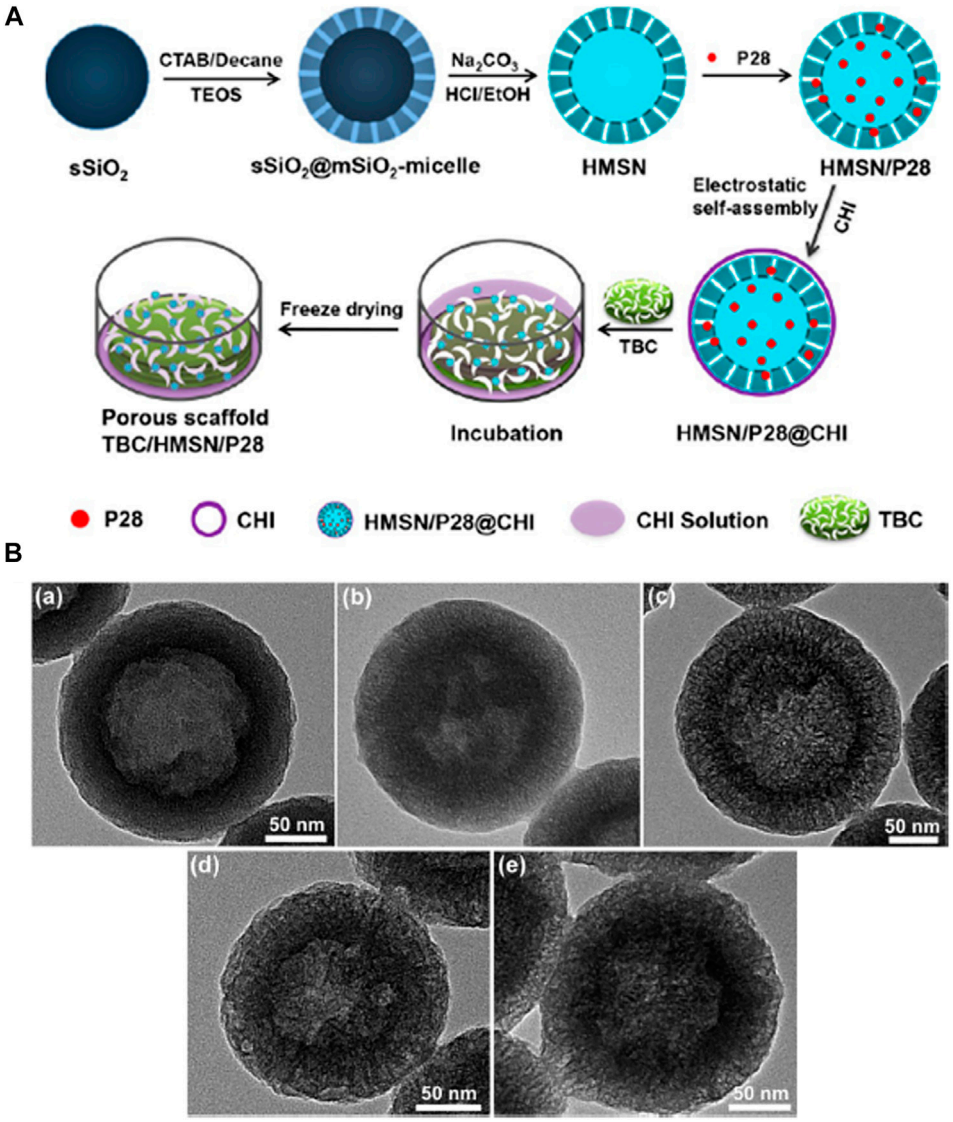

FIGURE 8 | (A) Illustration showing the synthetic procedure of the TBC/HMSN/P28 composite material. **(B)** TEM images of the HMSNs synthesized through varying molar ratios of decane/CTAB: a) 0.0, b) 0.5, c) 1.0, d) 2.0, and e) 4.0. Reprinted with permission from Cui et al. (2018). Copyright © 2017 American Chemical Society.

modified MCM41 particles were greater in size with a tendency to agglomerate. They exhibited highly ordered hexagonal arrays and streak structural features with 3 nm pore sizes indicating their mesoporous nature. The nanocomposites supported cell viability and the proliferation of MC3T3-E1 cells and, hence, should be further studied for bone repair tissue engineering applications.

MESOPOROUS SILICA NANOPARTICLES BASED BIOIMAGING OF BONE TISSUES

Although regenerative medicine is very promising where stem cell transplantation is employed to repair and regenerate along with drug delivery, there is a lacuna in monitoring the drug release at the site of injury. Hence, contrast agents can be functionalized onto the MSNs surface in order to have dual modalities like bioimaging and drug delivery.

Ren et al. (2017) developed a gadolinium (Gd) labelled defect-related luminescent MSN for bone marrow homing and enhanced osteogenic differentiation. This nanocomposite also aimed to achieve traceable drug delivery. Firstly, MSNs-COOH suspended in dimethyl sulfoxide (DMSO) were reacted with alendronates ALN for 24 h resulting in MSNs-ALN. Gd was conjugated to this to obtain MSN-ALN-Gd and MSNs-COOH-Gd. The monodispersed MSNs exhibited a walnut kernel morphology 100 nm in diameter with a mesoporous structure which is ideal for surface modification and drug loading. A sustained release of DEX was seen when loaded

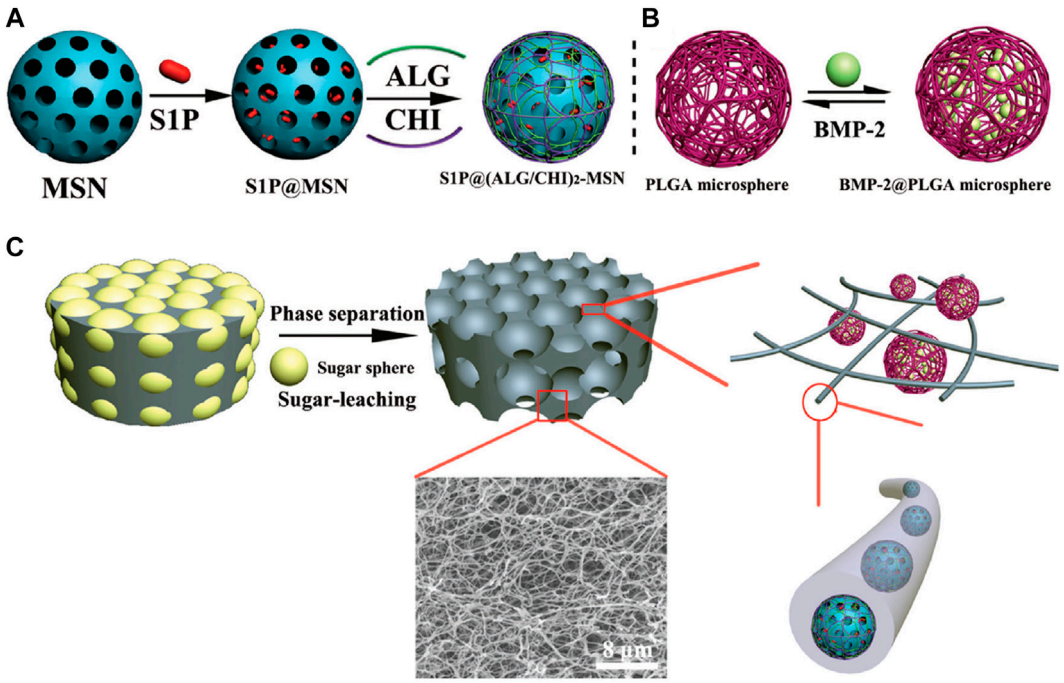

FIGURE 9 | Schematic presentation of the process to fabricate the bioactive factor loaded composite scaffold. **(A)** Schematic illustration of the preparation of S1P@$(ALG/CHI)_2$-MSNs; **(B)** the PLGA microspheres and BSA@PLGA microspheres; and **(C)** schematic illustration of the fabrication of the porous nanofibrous scaffold and the microstructure of the bioactive factor loaded composite scaffold. Reprinted with permission from Zhang et al. (2018). Copyright © The Royal Society of Chemistry 2018.

into nanocarriers while effective monitoring of drug release was attributed to the unique defect-related luminescent property. The nanocarriers with superior biocompatibility were taken up by BMSCs by an energy-dependent macropinocytosis pathway. After internalization, the MSN-ALN-Gd nanocomposites were distributed in the lysosomes.

ALN modification resulted in the enhanced accumulation of MSN-ALN-Gd in bone confirming their promise for targeted drug delivery to bone tissues. The MSN-ALN-Gd further showed high relaxivity due to the covalently bonding of Gd^{3+} to the interior pore or surface of the MSNs. Further, the dose dependent internalization of MSN-ALN-Gd was confirmed by the phantom images of BMSCs indicating its promising advantage towards both T1 and T2-weighted imaging. Drug release studies showed that the DEX@MSN-ALN-Gd system released 30% DEX over 24 h owing to an initial burst release. However, later a highly sustainable release was observed until 22 days. Enhanced ALP activity and calcium deposition in BMSCs upon treatment with the conjugates showed their significance in promoting bone tissue differentiation.

In another study, Li et al. (2018) fabricated biodegradable, photoluminescent and osteoinductive silica nanoparticles (SNs) reinforced with poly (citrate-siloxane) hybrid elastomers (PCS-SN). The composite was synthesized in two steps. The poly (citrate-siloxane) (PCS) was synthesized employing a one-pot thermal polymerization process using citric acid (CA), 1,8-octanediol (OD), and (3-aminopropyl) triethoxysilane (AS) with mol ratios of 1.0:1.0:0.2 at 140°C for 60 min. In the next step, the PCS-SN hybrid elastomers were fabricated by a direct hybridization of a PCS solution and silica-based sols, followed by further thermal crosslinking. PCS-SN hybrids showed a significantly rough surface with many spherical nanoparticles (500 nm size) in the PCS matrix. The density of spherical nanoparticles was directly proportional to the concentration of silica sol in the composite. PCS-SN showed an elongation at break of 60–80%. The tensile strength of PCS-SN hybrid elastomers ranged from 4.73 ± 0.24 to 9.37 ± 0.42 MPa. The increased tensile strength was attributed to the increased silica incorporation. The Young's modulus of the PCS-SN hybrid elastomer was in the range of 8.06 ± 0.34 to19.18 ± 0.78 MPa. Monodispersed spherical SNs were homogeneously dispersed in the PCS polymeric matrix. The elastomeric films exhibited a bright blue fluorescence under an excitation wavelength of 365 nm. Supplementation with SN resulted in an increase of the photoluminescent intensity at 425 nm. This property was used for long term fluorescent imaging performance *in vivo*. The biocompatible PCS-SN hybrid elastomers significantly facilitated the attachment and proliferation of an osteoblast cell line (MC3T3-E1).

ANTIBIOTIC FUNCTIONALIZED MESOPOROUS SILICA NANOPARTICLE

Post-operative infection is one of the critical problems that challenges the recovery and healing of bone injuries. Hence,

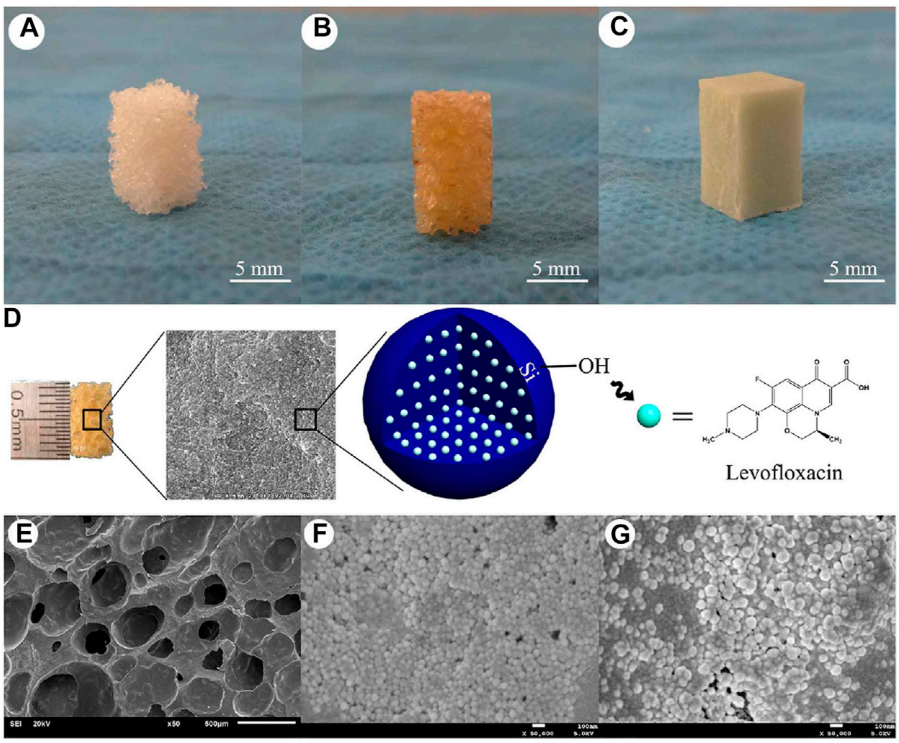

FIGURE 10 | The shape and internal structure of new synthetic composite scaffolds. The n-HA/PU composite porous scaffolds were manufactured using the situ foaming method. **(A)** The size of the material was 10 mm × 6 mm × 6 mm; **(B)** HA/PU scaffolds were combined with MSNs, which contained different concentrations of levofloxacin; **(C)** PMMA cement which contained 1 or 5 mg levofloxacin was used as a positive control group; **(D)** Levofloxacin was successfully loaded with mesoporous silica nanoparticle *via* electrostatic attraction; **(E)** Scanning electron micrographs of the n-HA/PU scaffold; **(F)** 1 mg Lev@MSNs/n-HA/PU; and **(G)** 5 mg Lev@MSNs/n-HA/PU. SEM micrographs of the n-HA/PU scaffold which has many pores **(E)**. It can be observed from the micrographs that there are many MSNs located on the walls of the macropores, which contain either 1 mg **(F)** or 5 mg **(G)** levofloxacin in each material. Reprinted from Wang et al. (2017). (Open access).

drug delivery using nanocomposites is one of the most powerful strategies that can induce osteogenesis as well as resist pathogenic infections at the site of injury. Zhou et al. (2018) fabricated a composite scaffold comprised of vancomycin (Van) loaded mesoporous silica nanoparticles (Van@MSNs) and a gelatin matrix. Initially, gelatin and Van@MSNs were mixed into a homogeneous solution which was then introduced into a mold and converted into a gel by keeping it at 4°C for 1 h. The resulting composites were highly porous with efficient compressibility which was attributed to the MSNs. The sustained release of Van from the nanocomposite resulted in superior inhibition of *Staphylococcus aureus* while it showed no adverse effects on the proliferation and differentiation of bone mesenchymal stem cells (BMSCs).

In addition, Wang et al. (2017) designed a levofloxacin loaded mesoporous silica microsphere/nanohydroxyapatite/polyurethane composite scaffold with promising therapeutic potential for chronic osteomyelitis with bone defects. Firstly, the scaffold was synthesized by reacting iron oxide (Fe_3O_4 in oleic acid) with cetyltrimethylammonium bromide (CTAB), sodium hydroxide (NaOH), ethyl acetate, and tetraethyl orthosilicate (TEOS) at 70°C for 3 h. Eventually the antibiotic, levofloxacin, was loaded onto the MSN *via* electrostatic attraction. Nanohydroxyapatite was further supplemented in the presence of polyethylene glycol (PEG400) as a surface dispersant. In the next step, polyurethane was incorporated into the above scaffold by *in situ* polymerization and a simultaneous foaming process. In this process, the reaction of the scaffolds with castor oil, isophorone diisocyanate, 1,4-butanediol, chitosan, and acetic acid resulted in the final product denoted as levofloxacin @ mesoporous silica nanoparticle/nano-hydroxyapatite/polyurethane (Lev@MSNs/n-HA/PU) as illustrated in **Figures 10A–D**. Morphologically, the scaffolds were porous and numerous micropores could be visualized on the walls of the macropores within the scaffolds that either contained 1 or 5 mg levofloxacin as seen in **Figures 10E–G**. A chronic osteomyelitis animal model using New Zealand White rabbits exhibited bone tissue swelling, decreased bone density, significant bone destruction, sequestrum formation, obscure boundaries, osteolytic lesions, and cortical thinning in the untreated group. On the other hand, complete bone cementation was observed when treated with the implants composed of 1 mg Lev@PMMA group and the 5 mg Lev@PMMA group as confirmed by X-ray images shown in **Figure 11**. The antibiotic loaded scaffolds significantly enhanced the formation of new bone trabeculae. Hence, such novel biomaterials may be used as a bacterial infection resistant implant material for bone tissue regeneration and healing.

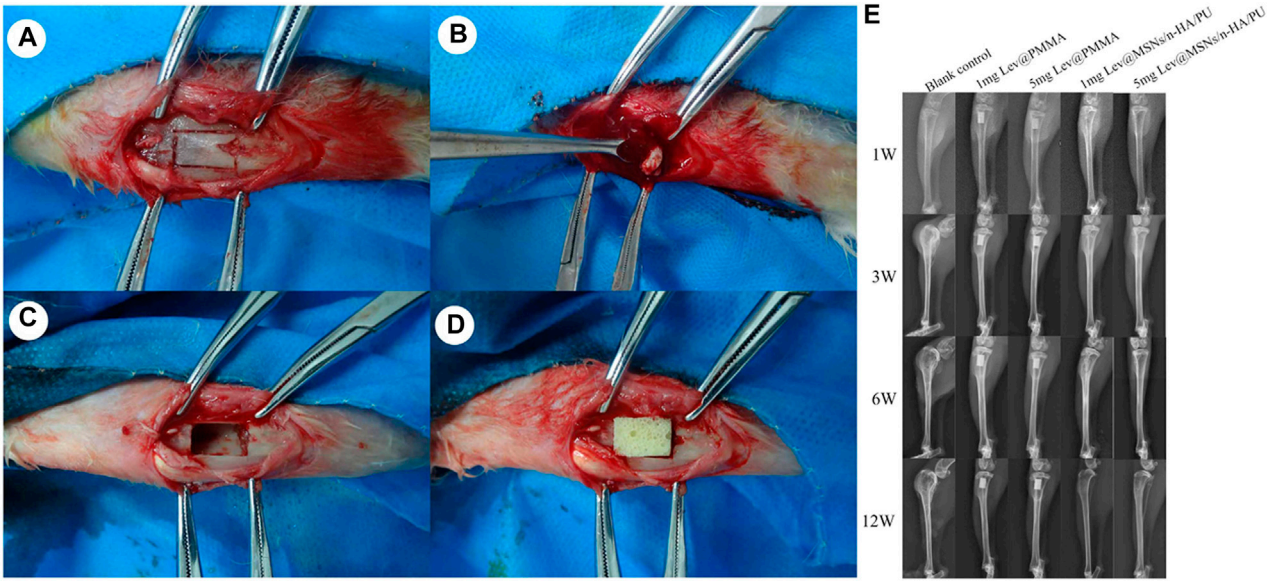

FIGURE 11 | The process of material implantation. **(A)** The cutting area was selected on the right side of proximal tibial; **(B)** Sequestrum, inflammatory tissue and purulence was debrided by using povidone iodine and normal saline; **(C)** After debridement, the size of the bone defects was 10 mm × 6 mm; **(D)** The new composite scaffolds was implanted in the bone defects; **(E)** Performance by X-ray imaging in each group at 3, 6, and 12 weeks, bone tissue swelling, decreased bone density, significant bone destruction, sequestrum formation, obscure boundary, osteolytic lesions, and cortical thinning were observed in the blank control group. No obvious osteomyelitis symptoms were observed in the 5 mg Lev@MSNs/n-HA/PU group. Reprinted from Wang et al. (2017). (Open access).

MESOPOROUS SILICA NANOPARTICLES BASED 3-DIMENSIONAL PRINTING

An important aspect of bone tissue engineering is to achieve osteogenic differentiation and osseointegration at the site of operation or implantation. Li et al. (2017) fabricated unique calcium phosphate cement (CPC)-based scaffolds combining the properties of mesoporous silica (MS) with recombinant human bone morphogenic protein-2 (rhBMP-2) that could effectively promote both vascularization and osteogenesis. Initially, CPC was mixed with 10 wt% MS to form a MS/CPC printing powder that was further mixed with a 10 wt% poly (vinyl) alcohol aqueous solution which acted as a binder. A 3D bioprinter was used to fabricate scaffolds with dimensions of φ 10 × 2 mm^3 and 3 × 4 × 15 mm^3 as seen in **Figures 12A–D**.

rhBMP-2 was further loaded onto the porous scaffolds by adding it drop-wise and letting it fully absorb for 4 h. The resulting scaffolds with pseudoplastic flow behavior were mesoporous with a narrow pore size distribution centred at 6.8 nm. MS/CPC/rhBMP-2 scaffolds enhanced the ALP-positive area and bone nodule formation upon treatment for 7 and 14 days confirming the osteogenic differentiation of hBMSCs. Moreover, a superior promotion of vascularization in rabbit femoral defects was observed after 4 weeks of implantation when the scaffolds were embedded in polymethylmethacrylate (PMMA) as seen in **Figures 12E–G**. Numerous blood vessels (red and yellow) were also visible inside the macropores of the MS/CPC/rhBMP-2 scaffolds (green) as illustrated in **Figures 12H–M**. Interestingly, the 3D printed scaffolds promoted excellent circumferential cortical regeneration where the newly formed bone gradually grew around and inside the scaffolds. After 12 weeks of implantation, the bone defects were re-bridged, providing an indication of effective repair and integration. Hence, these novel MS based scaffolds can modulate the tissue microenvironment for the promotion of osteogenic differentiation and vascularization possibly ensuring rapid recovery in the post-surgical phase.

FUTURE PERSPECTIVES

Although MSNs seem to be one of the most attractive nanomaterials for designing scaffolds for bone tissue regeneration, several key factors are needed to be considered in order to obtain a desired healing effect. The size and shape of the MSNs can be controlled by optimizing the reaction parameters such as pH, surfactant, silica precursor, and temperature. Altering the amount of an alkaline catalyst triethanolamine (TEA) during synthesis can fabricate MSNs with a controlled size in the range from 25 to 105 nm (Pan et al., 2012).

Moreover, the statistical Taguchi method can be employed for a systematic investigation into the reaction conditions in order to achieve uniform monodispersed MSNs. Parameters like pH, reaction time and TEOS content have a 57, 29, and 13% influence, respectively, on the size of resultant MSNs (Chiang et al., 2011). The rational use of surfactants, like CTAB and Brij-56, can direct the structure and shape evolution of the MSNs while propanetriol can be used as a cosolvent in aqueous solutions

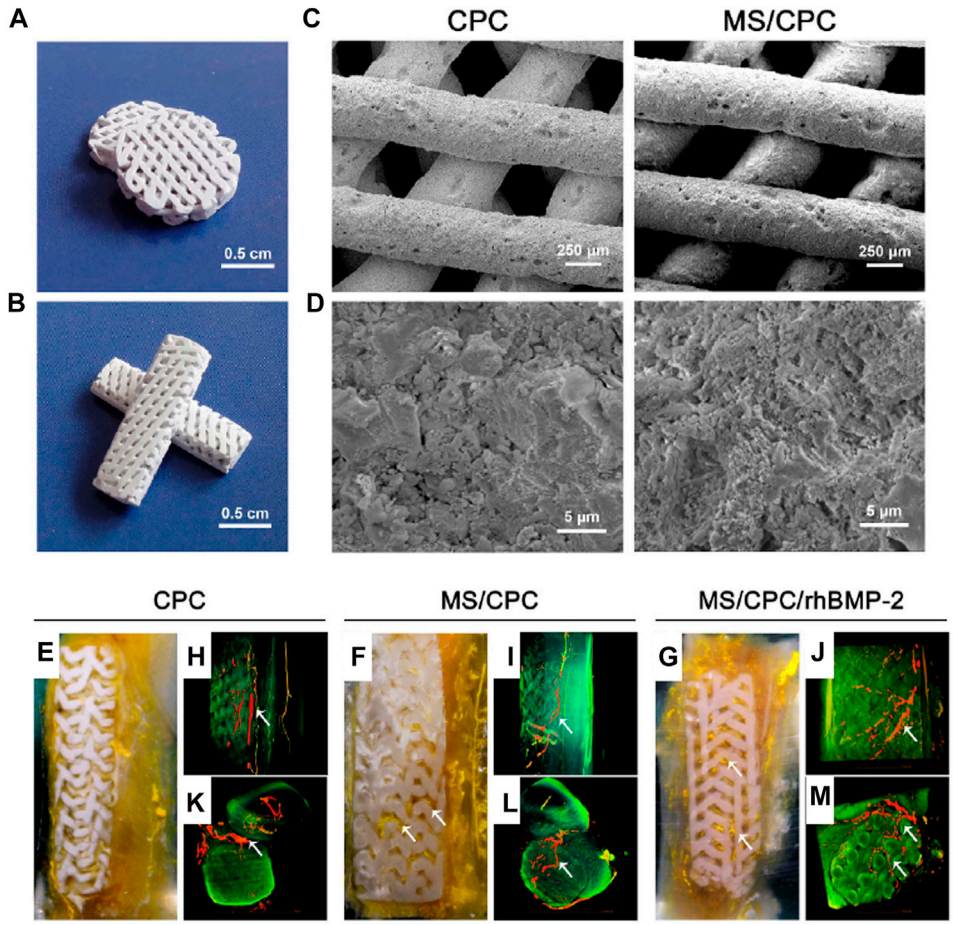

FIGURE 12 | Microstructure and morphology of the MS/CPC scaffolds. **(A,B)** Digital camera photographs of MS/CPC scaffolds for *in vitro* **(A)** and *in vivo* **(B)** experiments. Scanning electron micrographs of CPC and MS/CPC **(C)** ×150, **(D)** ×10 K; Effect of MS and rhBMP-2 release on vascularization. The **(E–G)** digital camera photographs of PMMA-embedded blocks from longitudinal sections and 3D reconstructed μ CT images of blood vessels from **(H–J)** the side view and **(K–M)** the top view of CPC, MS/CPC, and MS/CPC/rhBMP-2 scaffolds after 4 weeks of implantation. White arrow: newly formed blood vessels.

(He et al., 2009). Careful control of CTAB and ammonia concentration can be used to modify the length and width of rod shaped MSNs during synthesis employing the Stober method (Huang et al., 2010; Hao et al., 2012). Intrinsic doping with photosensitizers, such as chlorin e6 (Ce6), can also modulate the morphological features of the MSNs where the gradual transition of spheres to rods takes place (Yang et al., 2015).

The biomedical applications of MSNs area also dependent on its pore size. Infiltration of cells, cell adherence, cell proliferation, angiogenesis, neo-vasculature formation and the development of a tissue microenvironment is facilitated when using scaffolds with an optimal pore size.

Under alkaline conditions, CTAB can serve as a pore template resulting in 2–3 nm pore sizes in MSNs. Likewise, pore expanding agents like alkanes/ethanol, may enhance pore dimensions (Kao and Mou, 2013). Modification of an emulsion system can synthesize dendrimer-like MSNs with center-radial pore channels (Nandiyanto et al., 2009; Du and He, 2010; Zhang et al., 2010) while a microwave-assisted hydrothermal method can generate MSNs with a fibrous morphology (KCC-1) in microemulsion systems (Polshettiwar et al., 2010).

Like all other nanomaterials, the therapeutic property of MSNs is also dependent on surface chemistry. Drug release, biocompatibility, targeting, cell adherence, cell differentiation and osteogenesis can all be controlled by rationally tuning the surface properties of the MSNs incorporated within the scaffolds (Zhao et al., 2015). The high density of surface silanol groups also enables for easy functionalization with a group of diverse ligands on MSNs (Zhao et al., 2011). MCSs can be effectively targeted by conjugating hyaluronic acid (HA) onto the surface of MSNs (Huang et al., 2013). Similarly, arginine-glycine-aspartic acid (RGD) peptide-modification of MSNs may remarkably enhance cell adhesion on an alginate hydrogel compared to a MSNs-NH_2-incorporated hydrogel (Kehr et al., 2013). Therefore, rational surface functionalization of MSNs is critical to achieve desired therapeutic properties of such scaffolds for tissue engineering.

Another important aspect that should be addressed before the MSNs based nanoscaffolds can be introduced for medical use is

their biodegradability. The MSNs should be excreted from the organisms once their specific mission is accomplished. MSNs degradation can be achieved *via* three major steps. Firstly, the siloxane framework is hydrated in the aqueous media, while in the next step, the siloxanes are gradually hydrolyzed into silanols. Eventually, the nucleophilic attack of OH− leads to the leaching of silicic acid (Yamada et al., 2012). Hence, the surface area largely influences the rate of degradation. Spherical MSNs which degrade faster than rod shaped MSNs, can be incorporated while fabricating scaffolds or implants to ensure safety and removal after recovery (Hao et al., 2012). Other parameters, such as pore size, condensation degree, and surface functionalization of MSNs, also influence the extent and time required for degradation. Hence, more studies in simulated body fluids and even *in vivo* evaluation should be carried out to better understand the safety and shelf life of these scaffolds.

CONCLUSION

As this review has shown, MSNs provide an attractive solution for bone tissue regeneration due to their proven application in diverse types of scaffolds and implants. Their well studied properties like biodistribution, accumulation and excretion, make them suitable candidates for tissue engineering, drug delivery, and also bioimaging. The ease of surface functionalization of ligands and loading of bioactive compounds in the mesopores enable them to be used for both osteoinduction and differentiation. Several polymers like poly (L-lactic acid)/poly (ε-caprolactone), polylysine-modified polyethylenimine, poly (lactic-co-glycolic acid), and poly (citrate-siloxane) hybrid elastomers are widely used as linkers to functionalize fluorescent agents like FITC, peptides like BMP-2 and rhBMP-2, and drugs like DEX and β–estradiol (E2). Biogenic polymers like chitosan, gelatine and alginate are also used for surface modification for effective conjugation of oligonucleotides, calcium phosphate cement (CPC), nanohydroxyapatite, antibiotics (vancomycin and levofloxacin) and contrast agents (gadolinium). In view of the background, multifunctionalized MSNs can be considered as the next generation of theranostic agents that can simultaneously induce bone tissue regeneration, promote osseointegration, resist post-surgical pathogenic infections, and monitor the sustained release of drugs. Hence, MSN based scaffolds and implants can revolutionize medical science although pharmacokinetic, pharmacodynamic and toxicity profiles and should be thoroughly studied and established before entering healthcare.

AUTHOR CONTRIBUTIONS

SG and TW contributed equally in the conceptualization, manuscript preparation, corrections and editing.

ACKNOWLEDGMENTS

SG acknowledges the Department of Science and Technology (DST), Ministry of Science and Technology, Government of India and Jawaharlal Nehru Centre for Advanced Scientific Research, India for funding under the Post-doctoral Overseas Fellowship in Nano Science and Technology (Ref. JNC/AO/A.0610.1(4) 2019–2260 dated August 19, 2019).

REFERENCES

Amini, A. R., Laurencin, C. T., and Nukavarapu, S. P. (2012). Bone Tissue Engineering: Recent Advances and Challenges. *Crit. Rev. Biomed. Eng.* 40 (5), 363–408. doi:10.1615/critrevbiomedeng.v40.i5.10

Bao, C. L. M., Teo, E. Y., Chong, M. S., Liu, Y., Choolani, M., and Chan, J. K. (2013). *Advances in Bone Tissue Engineering, Regenerative Medicine and Tissue Engineering*. London, UK: InTech.

Chen, L., Zhou, X., and He, C. (2019). Mesoporous Silica Nanoparticles for Tissue-Engineering Applications. *Wiley Interdiscip. Rev. Nanomed Nanobiotechnol.* 11, e1573. doi:10.1002/wnan.1573

Chiang, Y.-D., Lian, H.-Y., Leo, S.-Y., Wang, S.-G., Yamauchi, Y., and Wu, K. C.-W. (2011). Controlling Particle Size and Structural Properties of Mesoporous Silica Nanoparticles Using the Taguchi Method. *J. Phys. Chem. C.* 115, 13158–13165. doi:10.1021/jp201017e

Croissant, J. G., Fatieiev, Y., Almalik, A., and Khashab, N. M. (2018). Mesoporous Silica and Organosilica Nanoparticles: Physical Chemistry, Biosafety, Delivery Strategies, and Biomedical Applications. *Adv. Healthc. Mater.* 7, 201700831. doi:10.1002/adhm.201700831

Cui, W., Liu, Q., Yang, L., Wang, K., Sun, T., Ji, Y., et al. (2018). Sustained Delivery of BMP-2-Related Peptide from the True Bone Ceramics/hollow Mesoporous Silica Nanoparticles Scaffold for Bone Tissue Regeneration. *ACS Biomater. Sci. Eng.* 4, 211–221. doi:10.1021/acsbiomaterials.7b00506

Dimitriou, R., Jones, E., McGonagle, D., and Giannoudis, P. V. (2011). Bone Regeneration: Current Concepts and Future Directions. *BMC Med.* 9 (1), 66. doi:10.1186/1741-7015-9-66

Dominici, M., Le Blanc, K., Mueller, I., Slaper-Cortenbach, I., Marini, F. C., Krause, D. S., et al. (2006). Minimal Criteria for Defining Multipotent Mesenchymal Stromal Cells. The International Society for Cellular Therapy Position Statement. *Cytotherapy*. 8 (4), 315–317. doi:10.1080/14653240600855905

Dragonas, P., Katsaros, T., Avila-Ortiz, G., Chambrone, L., Schiavo, J. H., and Palaiologou, A. (2019). Effects of Leukocyte-Platelet-Rich Fibrin (L-PRF) in Different Intraoral Bone Grafting Procedures: a Systematic Review. *Int. J. Oral Maxillofac. Surg.* 48, 250–262. doi:10.1016/j.ijom.2018.06.003

Du, X., and He, J. (2010). Fine-tuning of Silica Nanosphere Structure by Simple Regulation of the Volume Ratio of Cosolvents. *Langmuir*. 26, 10057–10062. doi:10.1021/la100196j

Enomoto, H., Furuichi, T., Zanma, A., Yamana, K., Yoshida, C., Sumitani, S., et al. (2004). Runx2 Deficiency in Chondrocytes Causes Adipogenic Changes *In Vitro*. *J. Cel Sci.* 117 (3), 417–425. doi:10.1242/jcs.00866

Finkemeier, C. G. (2002). Bone-grafting and Bone-Graft Substitutes. *J Bone Joint Surg Am.* 84 (3), 454–464. doi:10.2106/00004623-200203000-00020

Florencio-Silva, R., Sasso, G. R., Sasso-Cerri, E., Simões, M. J., and Cerri, P. S. (2015). Biology of Bone Tissue: Structure, Function, and Factors that Influence Bone Cells. *Biomed. Res. Int.* 2015, 421746. doi:10.1155/2015/421746

Gan, Q., Zhu, J., Yuan, Y., Liu, H., Qian, J., Li, Y., et al. (2015). A Dual-Delivery System of pH-Responsive Chitosan-Functionalized Mesoporous Silica Nanoparticles Bearing BMP-2 and Dexamethasone for Enhanced Bone Regeneration. *J. Mater. Chem. B.* 3, 2056–2066. doi:10.1039/c4tb01897d

Gaur, T., Lengner, C. J., Hovhannisyan, H., Bhat, R. A., Bodine, P. V. N., Komm, B. S., et al. (2005). Canonical WNT Signaling Promotes Osteogenesis by Directly Stimulating Runx2 Gene Expression. *J. Biol. Chem.* 280 (39), 33132–33140. doi:10.1074/jbc.m500608200

Gupta, A., Leong, D. T., Bai, H. F., Singh, S. B., Lim, T.-C., and Hutmacher, D. W. (2007). Osteo-maturation of Adipose-Derived Stem Cells Required the Combined Action of Vitamin D3, β-glycerophosphate, and Ascorbic Acid. *Biochem. Biophysical Res. Commun.* 362, 17–24. doi:10.1016/j.bbrc.2007.07.112

Hao, N., Liu, H., Li, L., Chen, D., Li, L., and Tang, F. (2012). *In Vitro* degradation Behavior of Silica Nanoparticles under Physiological Conditions. *J. Nanosci. Nanotechnol.* 12, 6346–6354. doi:10.1166/jnn.2012.6199

Harada, S.-i., and Rodan, G. A. (2003). Control of Osteoblast Function and Regulation of Bone Mass. *Nature*. 423 (6937), 349–355. doi:10.1038/nature01660

He, Q., Cui, X., Cui, F., Guo, L., and Shi, J. (2009). Size-controlled Synthesis of Monodispersed Mesoporous Silica Nano-Spheres under a Neutral Condition. *Microporous Mesoporous Mater.* 117, 609–616. doi:10.1016/j.micromeso.2008.08.004

Henstock, J. R., Canham, L. T., and Anderson, S. I. (2015). Silicon: The Evolution of its Use in Biomaterials. *Acta Biomater.* 11, 17–26. doi:10.1016/j.actbio.2014.09.025

Hess, R., Douglas, T., Myers, K. A., Rentsch, B., Rentsch, C., Worch, H., et al. (2010). Hydrostatic Pressure Stimulation of Human Mesenchymal Stem Cells Seeded on Collagen-Based Artificial Extracellular Matrices. *J. Biomech. Eng.* 132 (2), 021001–021006. doi:10.1115/1.4000194

Hickey, D. J., Ercan, B., Sun, L., and Webster, T. J. (2015). Adding MgO Nanoparticles to Hydroxyapatite-PLLA Nanocomposites for Improved Bone Tissue Engineering Applications. *Acta Biomater.* 14, 175–184. doi:10.1016/j.actbio.2014.12.004

Hu, Y., Cai, K., Luo, Z., and Jandt, K. D. (2010). Layer-By-Layer Assembly of β-Estradiol Loaded Mesoporous Silica Nanoparticles on Titanium Substrates and its Implication for Bone Homeostasis. *Adv. Mater.* 22, 4146–4150. doi:10.1002/adma.201000854

Huang, X., Li, L., Liu, T., Hao, N., Liu, H., Chen, D., et al. (2011). The Shape Effect of Mesoporous Silica Nanoparticles on Biodistribution, Clearance, and Biocompatibility *In Vivo*. *ACS Nano*. 5, 5390–5399. doi:10.1021/nn200365a

Huang, X., Teng, X., Chen, D., Tang, F., and He, J. (2010). The Effect of the Shape of Mesoporous Silica Nanoparticles on Cellular Uptake and Cell Function. *Biomaterials*. 31, 438–448. doi:10.1016/j.biomaterials.2009.09.060

Huang, X., Zhang, F., Wang, H., Niu, G., Choi, K. Y., Swierczewska, M., et al. (2013). Mesenchymal Stem Cell-Based Cell Engineering with Multifunctional Mesoporous Silica Nanoparticles for Tumor Delivery. *Biomaterials*. 34, 1772–1780. doi:10.1016/j.biomaterials.2012.11.032

Igarashi, M., Kamiya, N., Hasegawa, M., Kasuya, T., Takahashi, T., and Takagi, M. (2004). Inductive Effects of Dexamethasone on the Gene Expression of Cbfa1, Osterix and Bone Matrix Proteins during Differentiation of Cultured Primary Rat Osteoblasts. *J. Mol. Histol.* 35 (1), 3–10. doi:10.1023/b:hijo.0000020883.33256.fe

Jansen, J. H., Van Der Jagt, O. P., Punt, B. J., Verhaar, J. A., van Leeuwen, J. P., Weinans, H., et al. (2010). Stimulation of Osteogenic Differentiation in Human Osteoprogenitor Cells by Pulsed Electromagnetic fields: an *In Vitro* Study. *BMC Musculoskelet. Disord.* 11, 188. doi:10.1186/1471-2474-11-188

Kao, K.-C., and Mou, C.-Y. (2013). Pore-expanded Mesoporous Silica Nanoparticles with Alkanes/ethanol as Pore Expanding Agent. *Microporous Mesoporous Mater.* 169, 7–15. doi:10.1016/j.micromeso.2012.09.030

Kargozar, S., Singh, R. K., Kim, H.-W., and Baino, F. (2020). "Hard" Ceramics for "Soft" Tissue Engineering: Paradox or Opportunity?. *Acta Biomater.* 115, 1–28. doi:10.1016/j.actbio.2020.08.014

Kehr, N. S., Prasetyanto, E. A., Benson, K., Ergün, B., Galstyan, A., and Galla, H.-J. (2013). Periodic Mesoporous Organosilica-Based Nanocomposite Hydrogels as Three-Dimensional Scaffolds. *Angew. Chem. Int. Ed.* 52, 1156–1160. doi:10.1002/anie.201206951

Komori, T. (2006). Regulation of Osteoblast Differentiation by Transcription Factors. *J. Cel. Biochem.* 99 (5), 1233–1239. doi:10.1002/jcb.20958

Lee, K.-S., Kim, H.-J., Li, Q.-L., Chi, X.-Z., Ueta, C., Komori, T., et al. (2000). Runx2 Is a Common Target of Transforming Growth Factor β1 and Bone Morphogenetic Protein 2, and Cooperation between Runx2 and Smad5 Induces Osteoblast-specific Gene Expression in the Pluripotent Mesenchymal Precursor Cell Line C2C12. *Mol. Cel. Biol.* 20 (23), 8783–8792. doi:10.1128/mcb.20.23.8783-8792.2000

Lee, M.-H., Kim, Y.-J., Kim, H.-J., Park, H.-D., Kang, A.-R., Kyung, H.-M., et al. (2003). BMP-2-induced Runx2 Expression Is Mediated by Dlx5, and TGF-B1 Opposes the BMP-2-Induced Osteoblast Differentiation by Suppression of Dlx5 Expression. *J. Biol. Chem.* 278 (36), 34387–34394. doi:10.1074/jbc.m211386200

Li, C., Jiang, C., Deng, Y., Li, T., Li, N., Peng, M., et al. (2017). RhBMP-2 Loaded 3D-Printed Mesoporous Silica/calcium Phosphate Cement Porous Scaffolds with Enhanced Vascularization and Osteogenesis Properties. *Sci. Rep.* 7, 41331. doi:10.1038/srep41331

Li, Y., Guo, Y., Ge, J., Ma, P. X., and Lei, B. (2018). *In Situ* silica Nanoparticles-Reinforced Biodegradable Poly(citrate-Siloxane) Hybrid Elastomers with Multifunctional Properties for Simultaneous Bioimaging and Bone Tissue Regeneration. *Appl. Mater. Today*. 10, 153–163. doi:10.1016/j.apmt.2017.11.007

Liu, W., Toyosawa, S., Furuichi, T., Kanatani, N., Yoshida, C., Liu, Y., et al. (2001). Overexpression of Cbfa1 in Osteoblasts Inhibits Osteoblast Maturation and Causes Osteopenia with Multiple Fractures. *J. Cel Biol.* 155 (1), 157–166. doi:10.1083/jcb.200105052

Lu, F., Wu, S.-H., Hung, Y., and Mou, C.-Y. (2009). Size Effect on Cell Uptake in Well-Suspended, Uniform Mesoporous Silica Nanoparticles. *Small*. 5, 1408–1413. doi:10.1002/smll.200900005

Mahapatra, C., Singh, R. K., Kim, J.-J., Patel, K. D., Perez, R. A., Jang, J.-H., et al. (2016). Osteopromoting Reservoir of Stem Cells: Bioactive Mesoporous Nanocarrier/collagen Gel through Slow-Releasing FGF18 and the Activated BMP Signaling. *ACS Appl. Mater. Inter.* 8, 27573–27584. doi:10.1021/acsami.6b09769

Mishra, R., Bishop, T., Valerio, I. L., Fisher, J. P., and Dean, D. (2016). The Potential Impact of Bone Tissue Engineering in the Clinic. *Regenerative Med.* 11 (6), 571–587. doi:10.2217/rme-2016-0042

Nakashima, K., Zhou, X., Kunkel, G., Zhang, Z., Deng, J. M., Behringer, R. R., et al. (2002). The Novel Zinc finger-containing Transcription Factor Osterix Is Required for Osteoblast Differentiation and Bone Formation. *Cell.* 108 (1), 17–29. doi:10.1016/s0092-8674(01)00622-5

Nandiyanto, A. B. D., Kim, S.-G., Iskandar, F., and Okuyama, K. (2009). Synthesis of Spherical Mesoporous Silica Nanoparticles with Nanometer-Size Controllable Pores and Outer Diameters. *Microporous Mesoporous Mater.* 120, 447–453. doi:10.1016/j.micromeso.2008.12.019

O'Keefe, R. J., and Mao, J. (2011). Bone Tissue Engineering and Regeneration: from Discovery to the Clinic—An Overview. *Tissue Eng. B Rev.* 17 (6), 389–392. doi:10.1089/ten.TEB2011.0475

Padmanabhan, J., and Kyriakides, T. R. (2015). Nanomaterials, Inflammation, and Tissue Engineering. *WIREs Nanomed Nanobiotechnol.* 7, 355–370. doi:10.1002/wnan.1320

Pan, L., He, Q., Liu, J., Chen, Y., Ma, M., Zhang, L., et al. (2012). Nuclear-targeted Drug Delivery of TAT Peptide-Conjugated Monodisperse Mesoporous Silica Nanoparticles. *J. Am. Chem. Soc.* 134, 5722–5725. doi:10.1021/ja211035w

Pavlin, D., Dove, S. B., Zadro, R., and Gluhak-Heinrich, J. (2000). Mechanical Loading Stimulates Differentiation of Periodontal Osteoblasts in a Mouse Osteoinduction Model: Effect on Type I Collagen and Alkaline Phosphatase Genes. *Calcif. Tissue Int.* 67 (2), 163–172. doi:10.1007/s00223001105

Pavlin, D., Zadro, R., and Gluhak-Heinrich, J. (2001). Temporal Pattern of Stimulation of Osteoblast-Associated Genes during Mechanically-Induced OsteogenesisIn Vivo: Early Responses of Osteocalcin and Type I Collagen. *Connect. Tissue Res.* 42 (2), 135–148. doi:10.3109/03008200109014255

Perez, R. A., Singh, R. K., Kim, T.-H., and Kim, H.-W. (2017). Silica-based Multifunctional Nanodelivery Systems toward Regenerative Medicine. *Mater. Horiz.* 4, 772–799. doi:10.1039/c7mh00017k

Polshettiwar, V., Cha, D., Zhang, X., and Basset, J. M. (2010). High-surface-area Silica Nanospheres (KCC-1) with a Fibrous Morphology. *Angew. Chem. Int. Ed.* 49, 9652–9656. doi:10.1002/anie.201003451

Qiu, K., Chen, B., Nie, W., Zhou, X., Feng, W., Wang, W., et al. (2016). Electrophoretic Deposition of Dexamethasone-Loaded Mesoporous Silica Nanoparticles onto Poly(l-Lactic Acid)/Poly(ε-Caprolactone) Composite Scaffold for Bone Tissue Engineering. *ACS Appl. Mater. Inter.* 8, 4137–4148. doi:10.1021/acsami.5b11879

Rahikkala, A., Pereira, S. A. P., Figueiredo, P., Passos, M. L. C., Araujo, A. R. T. S., Saraiva, M. L. M. F. S., et al. (2018). Mesoporous Silica Nanoparticles for Targeted and Stimuli-Responsive Delivery of Chemotherapeutics: A Review. *Adv. Biosyst.* 2, 201800020. doi:10.1002/adbi.201800020

Ren, H., Chen, S., Jin, Y., Zhang, C., Yang, X., Ge, K., et al. (2017). A Traceable and Bone-Targeted Nanoassembly Based on Defect-Related Luminescent Mesoporous Silica for Enhanced Osteogenic Differentiation. *J. Mater. Chem. B.* 5, 1585–1593. doi:10.1039/c6tb02552h

Singh, R. K., Jin, G.-Z., Mahapatra, C., Patel, K. D., Chrzanowski, W., and Kim, H.-W. (2015). Mesoporous Silica-Layered Biopolymer Hybrid Nanofibrous

Scaffold: A Novel Nanobiomatrix Platform for Therapeutics Delivery and Bone Regeneration. *ACS Appl. Mater. Inter.* 7, 8088–8098. doi:10.1021/acsami.5b00692

Vallhov, H., Gabrielsson, S., Strømme, M., Scheynius, A., and Garcia-Bennett, A. E. (2007). Mesoporous Silica Particles Induce Size Dependent Effects on Human Dendritic Cells. *Nano Lett.* 7, 3576–3582. doi:10.1021/nl0714785

Wang, J., Yu, J., Yan, Y., Yang, D., Wang, P., Xu, Y., et al. (2019). Biodegradable Polyester/modified Mesoporous Silica Composites for Effective Bone Repair with Self-reinforced Properties. *Polym. Adv. Technol.* 30, 1461–1472. doi:10.1002/pat.4578

Wang, Q., Chen, C., Liu, W., He, X., Zhou, N., Zhang, D., et al. (2017). Levofloxacin Loaded Mesoporous Silica Microspheres/nano-Hydroxyapatite/polyurethane Composite Scaffold for the Treatment of Chronic Osteomyelitis with Bone Defects. *Sci. Rep.* 7, 41808. doi:10.1038/srep41808

Wu, S., Liu, X., Yeung, K. W. K., Liu, C., and Yang, X. (2014). Biomimetic Porous Scaffolds for Bone Tissue Engineering. *Mater. Sci. Eng. R: Rep.* 80, 1–36. doi:10.1016/j.mser.2014.04.001

Yamada, H., Urata, C., Aoyama, Y., Osada, S., Yamauchi, Y., and Kuroda, K. (2012). Preparation of Colloidal Mesoporous Silica Nanoparticles with Different Diameters and Their Unique Degradation Behavior in Static Aqueous Systems. *Chem. Mater.* 24, 1462–1471. doi:10.1021/cm3001688

Yang, G., Gong, H., Qian, X., Tan, P., Li, Z., Liu, T., et al. (2015). Mesoporous Silica Nanorods Intrinsically Doped with Photosensitizers as a Multifunctional Drug Carrier for Combination Therapy of Cancer. *Nano Res.* 8, 751–764. doi:10.1007/s12274-014-0558-0

Yaszemski, M., Payne, R. G., Hayes, W. C., Langer, R., and Mikos, A. G. (1996). Evolution of Bone Transplantation: Molecular, Cellular and Tissue Strategies to Engineer Human Bone. *Biomaterials*. 17 (2), 175–185. doi:10.1016/0142-9612(96)85762-0

Yourek, G., McCormick, S. M., Mao, J. J., and Reilly, G. C. (2010). Shear Stress Induces Osteogenic Differentiation of Human Mesenchymal Stem Cells. *Regenerative Med.* 5 (5), 713–724. doi:10.2217/rme.10.60

Zhang, H., Li, Z., Xu, P., Wu, R., and Jiao, Z. (2010). A Facile Two Step Synthesis of Novel Chrysanthemum-like Mesoporous Silica Nanoparticles for Controlled Pyrene Release. *Chem. Commun.* 46, 6783–6785. doi:10.1039/c0cc01673j

Zhang, Q., Qin, M., Zhou, X., Nie, W., Wang, W., Li, L., et al. (2018). Porous Nanofibrous Scaffold Incorporated with S1P Loaded Mesoporous Silica Nanoparticles and BMP-2 Encapsulated PLGA Microspheres for Enhancing Angiogenesis and Osteogenesis. *J. Mater. Chem. B* 6, 6731–6743. doi:10.1039/c8tb02138d

Zhao, X., Yuan, Z., Yildirimer, L., Zhao, J., Lin, Z. Y. W., Cao, Z., et al. (2015). Tumor-triggered Controlled Drug Release from Electrospun Fibers Using Inorganic Caps for Inhibiting Cancer Relapse. *Small* 11, 4284–4291. doi:10.1002/smll.201500985

Zhao, Y., Sun, X., Zhang, G., Trewyn, B. G., Slowing, I. I., and Lin, V. S.-Y. (2011). Interaction of Mesoporous Silica Nanoparticles with Human Red Blood Cell Membranes: Size and Surface Effects. *ACS Nano* 5, 1366–1375. doi:10.1021/nn103077k

Zhou, X., Feng, W., Qiu, K., Chen, L., Wang, W., Nie, W., et al. (2015). BMP-2 Derived Peptide and Dexamethasone Incorporated Mesoporous Silica Nanoparticles for Enhanced Osteogenic Differentiation of Bone Mesenchymal Stem Cells. *ACS Appl. Mater. Inter.* 7, 15777–15789. doi:10.1021/acsami.5b02636

Zhou, X., Weng, W., Chen, B., Feng, W., Wang, W., Nie, W., et al. (2018). Mesoporous Silica Nanoparticles/gelatin Porous Composite Scaffolds with Localized and Sustained Release of Vancomycin for Treatment of Infected Bone Defects. *J. Mater. Chem. B.* 6, 740–752. doi:10.1039/c7tb01246b

Zhou, X., Zhang, Q., Chen, L., Nie, W., Wang, W., Wang, H., et al. (2019). Versatile Nanocarrier Based on Functionalized Mesoporous Silica Nanoparticles to Codeliver Osteogenic Gene and Drug for Enhanced Osteodifferentiation. *ACS Biomater. Sci. Eng.* 5, 710–723. doi:10.1021/acsbiomaterials.8b01110

Conflict of Interest: The authors declare that the research was conducted in the absence of any commercial or financial relationships that could be construed as a potential conflict of interest.